



This is a repository copy of *Evidence for orbital and North Atlantic climate forcing in alpine Southern California between 125 and 10 ka from multi-proxy analyses of Baldwin Lake*.

White Rose Research Online URL for this paper:  
<http://eprints.whiterose.ac.uk/117010/>

Version: Accepted Version

---

**Article:**

Glover, K.C. [orcid.org/0000-0002-1616-0215](https://orcid.org/0000-0002-1616-0215), MacDonald, G.M., Kirby, M.E. et al. (5 more authors) (2017) Evidence for orbital and North Atlantic climate forcing in alpine Southern California between 125 and 10 ka from multi-proxy analyses of Baldwin Lake. *Quaternary Science Reviews*, 167. pp. 47-62. ISSN 0277-3791

<https://doi.org/10.1016/j.quascirev.2017.04.028>

---

Article available under the terms of the CC-BY-NC-ND licence  
(<https://creativecommons.org/licenses/by-nc-nd/4.0/>)

**Reuse**

This article is distributed under the terms of the Creative Commons Attribution-NonCommercial-NoDerivs (CC BY-NC-ND) licence. This licence only allows you to download this work and share it with others as long as you credit the authors, but you can't change the article in any way or use it commercially. More information and the full terms of the licence here: <https://creativecommons.org/licenses/>

**Takedown**

If you consider content in White Rose Research Online to be in breach of UK law, please notify us by emailing [eprints@whiterose.ac.uk](mailto:eprints@whiterose.ac.uk) including the URL of the record and the reason for the withdrawal request.



[eprints@whiterose.ac.uk](mailto:eprints@whiterose.ac.uk)  
<https://eprints.whiterose.ac.uk/>

1 **ABSTRACT**

2 We employed a new, multi-proxy record from Baldwin Lake (~125 - 10 ka) to examine drivers  
3 of terrestrial Southern California climate over long timescales. Correlated bulk organic and  
4 biogenic silica proxy data demonstrated high-amplitude changes from 125 - 71 ka, suggesting  
5 that summer insolation directly influenced lake productivity during MIS 5. From 60 - 57 ka,  
6 hydrologic state changes and events occurred in California and the U.S. Southwest, though the  
7 pattern of response varied geographically. Intermediate, less variable levels of winter and  
8 summer insolation followed during MIS 3 (57 - 29 ka), which likely maintained moist conditions  
9 in Southern California that were punctuated with smaller-order, millennial-scale events. These  
10 Dansgaard-Oeschger events brought enhanced surface temperatures (SSTs) to the eastern Pacific  
11 margin, and aridity to sensitive terrestrial sites in the Southwest and Southern California. Low  
12 temperatures and reduced evaporation are widespread during MIS 2, though there is increasing  
13 evidence for moisture extremes in Southern California from 29 - 20 ka. Our record shows that  
14 both orbital-scale radiative forcing and rapid North Atlantic temperature perturbations were  
15 likely influences on Southern California climate prior to the last glacial. However, these forcings  
16 produced a hydroclimatic response throughout California and the U.S. Southwest that was  
17 geographically complex. This work highlights that it is especially urgent to improve our  
18 understanding of the response to rapid climatic change in these regions. Enhanced temperature  
19 and aridity are projected for the rest of the 21<sup>st</sup> century, which will place stress on water  
20 resources.

21

22

23

## 24 **1. Introduction**

25 Throughout the U.S. Southwest, Great Basin, and California, climate model projections for the  
26 21st century indicate that increased radiative forcing that will produce enhanced temperatures,  
27 aridity, and climate variability (Overpeck et al., 2013). These projections prompted our  
28 investigation of regional sensitivity to past climate change and potential forcing mechanisms  
29 over the past 125 ka, in a sector of the U.S. that is already water-stressed and increasingly  
30 populous (Georgescu et al., 2012). Retrospective studies are crucial for deepening our  
31 understanding of large-scale climate dynamics and teleconnections, and assessing the potential  
32 range of temperature and hydrological variability. Long-lasting droughts in the West during the  
33 Late Quaternary have been documented (e.g. Brunelle and Anderson, 2003; Heusser et al., 2015;  
34 MacDonald and Case, 2005; Mensing et al., 2013), most of which were associated with warm  
35 intervals (Woodhouse et al., 2010). Conversely, extreme wet events were also a feature of West  
36 Coast climates (e.g. Bird and Kirby, 2006; Kirby et al., 2013, 2012). These prolonged  
37 hydroclimatic events, on the order of several decades or centuries, have no analogue in the past  
38 150 years of instrumental records.

39  
40 A growing body of climatic records from the U.S. Southwest, Great Basin, and Southern  
41 California suggests regional sensitivity to a variety of climate drivers that include an  
42 atmospheric-oceanic teleconnection with the North Atlantic (Asmerom et al., 2010; MacDonald  
43 et al., 2008; Oster et al., 2014; Reheis et al., 2015; Wagner et al., 2010), Pacific Ocean (Hendy  
44 and Kennett, 2000a; Heusser, 1998; Lund and Mix, 1998) boreal insolation (Lachniet et al.,  
45 2014; Moseley et al., 2016), and migrating storm tracks (Garcia et al., 2014; Kirby et al., 2006;  
46 Owen et al., 2003). Offshore marine cores have documented long histories through several  
47 Marine Isotope Stages (MISs), but with dynamically different responses compared to terrestrial

48 sites (Heusser and Basalm, 1977; Hooghiemstra et al., 2006). The longer-term climate history of  
49 terrestrial Southern California throughout past glaciations and multiple MISs is lesser-known,  
50 compared to abundant studies on the Holocene and last glacial (MIS 2).

51

52 In this study, a newly-acquired core from Baldwin Lake in the San Bernardino Mountains (SBM)  
53 that spanned 125 – 10 ka provided insight to the long-term temperature and hydrological  
54 variability of Southern California, and associated climatic drivers. We use this material to  
55 address the following questions: Is alpine Southern California sensitive to orbital and North  
56 Atlantic forcing over long timescales? How does the record of paleoenvironmental change and  
57 climatic variability at Baldwin Lake compare to other Southern California, Great Basin and  
58 Southwestern sites over the past 125 – 20 ka?

59

## 60 **2. Setting**

61 Located east of the Los Angeles Basin, the SBM are part of the Transverse Ranges and include  
62 some of the highest elevation peaks in Southern California. The SBM form a barrier between the  
63 interior Mojave and Sonoran Deserts, and the summer-dry, winter-wet Mediterranean conditions  
64 towards the coast. The San Andreas and Mill Creek Faults bound either side of the SBM range.  
65 Triassic- to Cretaceous-age granitic rocks dominate the SBM range (Morton and Miller, 2006),  
66 with other allocthonous sedimentary terranes of Precambrian and Mesozoic age (Dibblee, 1964).  
67 High relief valleys and slopes are often covered with Quaternary deposits, including alluvium,  
68 talus, and fanglomerates.

69

70 Baldwin Lake (34.275°N, 116.8°W) lies at an elevation of 2060 m in the Big Bear Valley of the  
71 SBM, approximately 160 km east of the Pacific coastline (Figure 1). It is presently an

72 intermittent lake, and one of two major lake basins in Big Bear Valley, with a 79 km<sup>2</sup> watershed  
73 (Big Bear Lake TMDL Task Force, 2012). To the west, the Big Bear Lake watershed is 96 km<sup>2</sup>,  
74 and supported a lake throughout the Holocene (Kirby et al., 2012; Paladino, 2008). Sugarloaf  
75 Mountain to the south (3033 m) is the primary sediment source of the Baldwin basin, via the 14  
76 km<sup>2</sup> Sugarloaf fan (Flint and Martin, 2012; Leidy, 2006). Smaller-scale faults occur throughout  
77 Big Bear Valley, including a thrust fault <1 km east of Baldwin Lake on Nelson Ridge (Flint and  
78 Martin, 2012). The highest elevations of the Transverse Ranges were glaciated during MIS 2;  
79 moraines still persist on the northern flank of Mt. San Gorgonio (3,506 masl) and mark later  
80 Holocene readvances (Owen et al., 2003).

81  
82 Mediterranean winter-wet and summer-dry conditions prevail throughout the SBM and Southern  
83 California, modulated by upwelling and currents on the North American Pacific margin. The  
84 configuration of the North Pacific High and North American Low, and westerly winds, drive this  
85 strong precipitation seasonality (Barron et al., 2003; Cayan and Peterson, 1989). Seasonal  
86 migration of the Polar Jet Stream (PJS) brings Pacific-derived moisture in the winter months, and  
87 Southern California's yearly precipitation averages 13 - 64 cm at lower elevations, and 64 – 150  
88 cm in the mountains ([www.wrh.noaa.gov](http://www.wrh.noaa.gov)). Annual precipitation averages are comparatively  
89 higher in Big Bear Valley, averaging ~220 cm/yr (U.S. Climate Data, 2016) and the moisture is  
90 largely derived from North Pacific winter storms (Wise, 2010). Other precipitation sources  
91 include orographic uplift, lateral snow drift (Minnich, 1984), and occasional summer storms that  
92 result from convection or dissipating tropical cyclones (Tubbs, 1972). Average July high  
93 temperature at Big Bear City is 27.2 °C, and January's average high is 8.3 °C (U.S. Climate Data,  
94 2016).

95

### 96 **3. Materials and Methods**

#### 97 3.1 Core recovery and Initial Core Description (ICD)

98 We re-cored Baldwin Lake in August 2012 at the basin depocenter (34°16.56633', -  
99 116°48.61182') with a CME-95 truck-mounted hollow stem auger drill. Prior coring at Baldwin  
100 Lake in 2004 yielded a 14.2 m sequence referred to as BLDC04-2 (Figure 1; Kirby et al., 2006).  
101 We refer to the new sequence of cores as BDL12, which consisted of overlapping 2.5 foot  
102 sections from two separate holes totaling 27m, now archived at UCLA. Cores were split at  
103 UCLA in 2013, then photographed and described at the Limnological Research Center (LRC) in  
104 2014, following conventions for Initial Core Description (ICD; Schnurrenberger et al., 2003).  
105 Key sedimentary structures and changes, described by depth from surface, have been  
106 summarized for the Supplemental Information.

107

#### 108 3.2 Sedimentary Analyses

109 Initial magnetic susceptibility data were collected at UCLA with a Bartington MS2e sensor, and  
110 later replicated at LRC. The GeoTek Multi-Sensor Core Logger at LRC collected 0.5-cm interval  
111 data. Loss-on-ignition (LOI) analysis at 1-cm intervals throughout BDL12 determined the bulk  
112 organic and carbonate content of the sediment (Dean, 1974; Heiri et al., 2001). Organic content  
113 was determined from the mass lost from 1-cm<sup>3</sup> volume samples after 1-hour burns at 550°C in a  
114 muffle furnace, and carbonate content was calculated after subsequent 1-hour burns at 950°C.  
115 Core density was calculated from sample dry weight values recorded during LOI analysis. Bulk  
116 inorganic values were percentage values, calculated from the remaining sample weight after all  
117 LOI burns compared to the initial dry weight. Mass accumulation rates (MARs) were calculated  
118 by multiplying a horizon's dry density by the sedimentation rate derived from the age model

119 (Rack et al., 1995). The 1-cm LOI and MS data were used to correlate the core sections, and  
120 determine a depth-below-surface value for each horizon of the sequence.

121  
122 Grain size sampling was initially done at 50 cm intervals (Silveira, 2014), with later sampling  
123 that targeted the basal coarse-grained facies, and the slowly-deposited MIS 2 interval. Samples  
124 (n=93) were digested in 30-35% H<sub>2</sub>O<sub>2</sub> to remove organics, then 1N HCl to remove carbonates,  
125 and lastly 1M NaOH to remove biogenic silicates, with intermittent centrifuging. Analyses were  
126 performed on a Malvern Mastersizer 2000 laser diffraction grain size analyzer at CSUF. The  
127 results were combined with high-resolution grain-size data from core BLDC04 (Blazevic et al.,  
128 2009) after re-aligning BLDC04's measured depths to correlate with BDL12 (see Supplemental  
129 Data). We reported the grain size mode (i.e., most frequently-occurring size) here in  $\mu\text{m}$ , after  
130 averaging values at 25-cm intervals for the core above 15 m, and at 50-cm intervals for the core  
131 section spanning 15 – 27 m. This was done to reduce noise and variable sampling resolutions  
132 throughout the ~27 m sequence. X-ray fluorescence (XRF) values were taken with a portable  
133 Innov-X Analyzer at 5 cm intervals along a split core surface that was lined with Ultralene film.  
134 Elements reported here include titanium (Ti), iron (Fe), calcium (Ca), potassium (K), and  
135 manganese (Mn).

### 136 137 3.3 Biogenic Silica (BSi)

138 We selectively analyzed biogenic silica (BSi) throughout the core in order to determine if lake  
139 productivity was a primary contributor to organic content changes. Amorphous silica is a  
140 structural component of diatoms, radiolarians, sponges, and phytoliths in aquatic environments  
141 Its measurement can potentially establish paleoproductivity and orbital influence in long lake  
142 histories (e.g. Prokopenko et al., 2006; Wohlfarth et al., 2008). Samples (n=32) from each of the

143 Marine Isotope Stages were analyzed with wet-alkaline extraction (Conley and Schelske, 2002)  
144 to characterize the relationship between organic content and BSi in different core facies.

145

#### 146 3.4 Chronologic control – assumptions and approach

147 We present a new age model here that extends to Marine Isotope Stage 5, and replaces the  
148 chronology of Kirby et al. (2006). The prior BLDC04-2 chronology included bulk dates that  
149 were not securely cross-dated with other methods, such as macrofossils or tephra layers  
150 (Zimmerman and Myrbo, 2015). From BDL12, AMS <sup>14</sup>C dating was conducted on seven wood  
151 and charcoal samples from the upper 8 m (Table 1). Infrared Stimulated Luminescence (IRSL)  
152 single-grain analysis was conducted on lower sections of the sequence that possessed a higher  
153 sand fraction (Buylaert et al., 2009; Rhodes, 2015). IRSL was applied to 150-175 μm K-feldspar  
154 grains, a technique increasingly used in Southern California, where quartz demonstrates low  
155 sensitivity in many locations (Garcia et al., 2014; Lawson et al., 2012). Four 20-cm sections of  
156 core were removed with a handsaw under luminescence laboratory lighting conditions, and a  
157 ~1.5 cm diameter cylinder of sediment was extracted from the core interior for IRSL dating.  
158 Once disturbed, these sections were not further analyzed. Preparation procedures, measurement  
159 at UCLA, and analysis followed Rhodes (2015). Fading measurements were used to correct both  
160 the IRSL signal measured at 50°C and the post-IR IRSL signal at 225°C, which demonstrated  
161 mean g-values of 0.03 and 0.015 respectively. Dose rates were calculated using ICP-MS (for U,  
162 Th) and ICP-OES (for K) determinations at SGS, Vancouver, Canada.

163

164 In order to construct the age model, we hypothesized that lake productivity was the primary  
165 contributor to total organic deposition and responded to changes in radiation. This was based



166 upon establishing relationships between key proxies, and making certain assumptions about  
167 basin response from the available data. First, we found that total organic matter and BSi data  
168 were correlated to each other ( $r=0.81$ ,  $p<0.001$ ) throughout the basin's history. This suggests that  
169 primary productivity, rather than preservation, was a key contributor to organic matter variation  
170 (Colman et al., 1995; Conley and Schelske, 2002; Kaplan et al., 2002). Second, we assume that  
171 local radiation is an important control on length of the freshwater photosynthetic season (e.g.  
172 Colman et al., 1995; Hu et al., 2003) and seasonal ice cover of the lake surface (McKay et al.,  
173 2008; Melles et al., 2006; Prokopenko et al., 2006). This assumption underlies our use of  
174 relatively local ( $30^{\circ}\text{N}$ ) summer insolation values as a proxy for seasonal light intensity, and  
175 primary driver for the associated peaks and troughs in total organic matter. This relationship  
176 between  $30^{\circ}\text{N}$  summer insolation and organic deposition was initially proposed for the site in the  
177 BLDC04-2 study (Kirby et al., 2006). The new organic matter dataset presented here replicated  
178 this apparent correlation to  $30^{\circ}\text{N}$  insolation in a 20-kyr section of core constrained with  
179 radiocarbon dating (40 – 20 ka).

180  
181 Visual curve matching (Groot et al., 2014) is a technique often used in the absence of other  
182 chronologic data or techniques (e.g. Tzedakis et al., 2001), or to supplement existing dates (e.g.  
183 Cacho et al., 1999). We employed it here it as a first-pass interpretation of basin response to  
184 climate drivers, and to construct a working age model for a newly-recovered long paleorecord. A  
185 series of tie points that match five peaks and troughs in the insolation and bulk organics datasets  
186 were established during MIS 5 (~116 – 71 ka; Table 1; Figure 2b). This exercise assumes that  
187 basin response to insolation shifts was immediate. While highly-resolved, directly-dated  
188 speleothem records spanning MIS 6 – 1 showed that Great Basin paleotemperature response

189 lagged boreal insolation shifts by ~3 kyr (Lachniet et al., 2014), there is not yet evidence for a  
190 similar lag at California sites. Age uncertainties from recent California paleorecords are  
191 comparatively greater (e.g. Herbert et al., 2001; Kirby et al., 2015; Oster and Kelley, 2016; this  
192 study). We ascribed a 2-kyr uncertainty to each tie-point for the Bacon 2.2 model (e.g. Mahan et  
193 al., 2014). This allowed for the possibility of 1) leads/lags in lake response compared to  
194 insolation, 2) influences other than temperature on organic matter production (e.g. nutrient  
195 cycling, moisture variability, and lake level variability), and 3) horizons where the tie-points  
196 overlapped with IRSL dates.

197  
198 Bacon 2.2 is a Bayesian approach to modeling the age of terrestrial cores (Blaauw and Christen,  
199 2011), and was employed for our age-depth model, incorporating  $^{14}\text{C}$  dates, 50°C and post-IR  
200 225°C luminescence dates, and five tie-points (Table 1, Figure 2). Bacon 2.2 algorithms perform  
201 calendar year conversions on  $^{14}\text{C}$  dates using IntCal13 (Reimer, 2013), and incorporate 2-sigma  
202 results in the model. In our model, the sediment mean accumulation rates was set to 50 cm/yr,  
203 and core section thickness was 50 cm, both suggested by the program (Blaauw and Christen,  
204 2011). Default priors for memory strength and memory mean (i.e., the degree to which  
205 sedimentation rate depends on that of adjacent horizons) were retained (Blaauw and Christen,  
206 2011; Goring et al., 2012). Luminescence sample J3096 was excluded, as it had low yield,  
207 displayed non-standard TL during preheat measurements, and was not in stratigraphic agreement  
208 with the other three samples (Table 1). A sharp break between clayey silt and the basal coarse-  
209 grained sandy layer downsection occurred at 2596 cm, possibly indicating of a hiatus. The  
210 uppermost lake sediments above 152 cm, where the youngest radiocarbon date was obtained,

211 have an uncertain age. Bacon 2.2 thus extrapolated the model between 0 – 152 cm without  
212 constraints.

213

## 214 **4. Results and Proxy**

### 215 4.1 Age Model

216 The weighted mean ages from the Bacon 2.2 age model (Figure 3) ranged from 125.7 – 5.3 ka  
217 cal BP, and were used for plotting figures, and the ensuing discussion of regional paleoclimate  
218 events. Without reliable age control above 152 cm, we were not confident that the Middle  
219 Holocene was the true age of the core top, and have excluded the desiccated upper 1 m of  
220 BDL12 from the ensuing figures and discussion. Direct dating of a charcoal fragment yielded a  
221 date of ~11.9 ka, and was obtained from a 3-cm charcoal layer (154-151 cm) not captured in the  
222 BLDC04-2 core. Previously, the upper material in the basin had been constrained by a ~20.3 ka  
223 bulk date at 114-117 cm (Kirby et al., 2006). Our new series of <sup>14</sup>C dates suggested, instead, that  
224 basin deposition continued after the Last Glacial Maximum (LGM) and included the Pleistocene-  
225 Holocene transition, though at very slow sedimentation rates (<0.03 cm/yr). The fading-corrected  
226 IRSL ages measured at 50°C and post-IR IRSL at 225°C were within range of the tie-points  
227 established (Table 1, Figure 2). The Bacon 2.2 age model (Figure 2), however, produced ages at  
228 the tie-point horizons that were 0.6 – 2.5 kyr offset from the ages initially assigned (Table 1).  
229 This was the result of assigning each a ±2 kyr error, and the influence of the IRSL dates in the  
230 model.

231

### 232 4.2 Sedimentology and Summary of Proxy Data

233 The BDL12 sequence was 91.9% complete, with some missing portions due to coring gaps and  
234 disturbances. Details of core stratigraphy are described by depth and approximate age in the

235 Supplemental Information. Key changes in core stratigraphy and sedimentological data (dry  
236 density, inorganics, MARs, and grain size) are shown by depth in Figure 3. Grain size mode  
237 results throughout the sequence were consistently in the range of silt (2-50  $\mu\text{m}$ ), except for the  
238 basal sand unit (mode  $>400 \mu\text{m}$ ). We summarized important sedimentological changes, as  
239 related to density and grain size, in Table 2 with the modifiers “sandy,” or “clayey” for cases  
240 when these size fractions were  $\geq 20\%$ , and the silt remained the dominant fraction ( $\geq 60\%$ ). Figure  
241 4 shows proxy data by age and MIS, with  $30^\circ\text{N}$  summer insolation shifts. MIS 5 substages are  
242 referenced with letters (e.g. MIS 5a), though age boundaries between substages have no global  
243 standard, and tend to vary geographically (Imbrie et al., 1984).

244

#### 245 4.3 Relationships and Environmental Interpretation for Baldwin Lake Proxy Data

246 We assumed the following relationships between proxy data, environmental conditions, and local  
247 summer insolation in our interpretation of site history. The immediate response for primary  
248 productivity to  $30^\circ\text{N}$  summer insolation during MIS 5 and MIS 3/2 was discussed in detail in  
249 section 3.4, as this assumption underpinned the age model. For Baldwin Lake, we interpreted  
250 positive correlation between BSi and total organic content as evidence that paleoproductivity was  
251 the dominant control on organic deposition. Several factors could have influenced the large  
252 changes observed in the coupled organic-BSi proxy data throughout the record. Correlated  
253 organic-BSi data have indicated shifts in lake water temperature at other high latitude or altitude  
254 sites (e.g. Blass et al., 2007; Hahn et al., 2013; McKay et al., 2008; Nussbaumer et al., 2011;  
255 Street et al., 2012; Vogel et al., 2013). High concentrations of BSi may also be linked to periods  
256 of increased runoff, and nutrients, within catchments (Ampel et al., 2008; Conley and Schelske,  
257 2002). Organic deposition as a proxy for relative wetness in the SBM has also been suggested,

258 with 30°N summer insolation impacting precipitation dynamics and moisture delivery to  
259 Southern California (Kirby et al., 2006). While it is challenging to disentangle how much each of  
260 these processes contributed to bulk organic measurements over time, key periods when one  
261 process seemed most dominant are discussed in the paleoenvironmental history of the basin  
262 below (section 5.1), with supporting evidence.

263  
264 Times of high organic deposition generally coincided with low values of both magnetic  
265 susceptibility and dry density (Table 2). Low MS values (<12 SI) throughout most of BDL12  
266 (Figure 4, Table 2) suggest this proxy detected a largely diamagnetic fraction throughout basin  
267 history (Dearing, 1999). Bedrock sources are largely granodioritic, yet the MS signal was  
268 dampened at times of episodic, high-energy clastic input. We hypothesized that in this basin,  
269 sediment frequently underwent sulfide reduction at the lake bottom, particularly when the lake  
270 was productive and organic deposition was  $\geq 10\%$ ). Such a reduction process can partially or  
271 completely dissolve magnetite, and produce low MS values (Dearing, 1999; Kirby et al., 2007;  
272 Nowaczyk et al., 2006).

273  
274 Trace element data aided our interpretation of allochthonous deposition, lake level changes, and  
275 lake ventilation. We interpreted relatively higher values of Ti, and in part, Fe, to phases of  
276 increased detrital, non-biogenic sediment deposition (Kylander et al., 2011; Vogel et al., 2013).  
277 Ca values changed in tandem with and were highly correlated to  $\text{CaCO}_3$  ( $r=0.84$ ; Figure 4h-i),  
278 suggesting that trace element Ca was largely derived from the precipitation of  $\text{CaCO}_3$ , rather  
279 than bedrock sources in the watershed. Such calcite precipitation tends to occur in lake systems  
280 when warm water temperatures, and potentially lake regression, produce saturation, leading to

281 high  $\text{CaCO}_3$  values (Hodell et al., 1998). High values in the manganese to titanium ratio (Mn:Ti;  
282 Figure 4) have been interpreted as a proxy for a well-mixed lake with bottom ventilation  
283 (Kylander et al., 2011). Times of high Ca,  $\text{CaCO}_3$  and Mn:Ti, including 114 – 107 ka, 87 – 75  
284 ka, and 14 – 10 ka (Figure 4), and were distinct facies, with lighter gray-brown sediment and,  
285 from 87 – 75 ka, horizons with mollusk shells. We interpreted the combination of increased Ca,  
286  $\text{CaCO}_3$ , and Mn:Ti to indicate phases when Baldwin Lake was warmer and well-ventilated. This  
287 warming may have also resulted from the lake shallowing. At horizons when all three of these  
288 parameters remained low, we assumed a stratified lake. When such conditions are coupled with  
289 high productivity, the deposition and bacterial decomposition of phytoplankton could produce  
290 reducing conditions and an anoxic lake bottom, and thus removal of a strong magnetic signal  
291 (Dearing, 1999).

292

## 293 **5. Discussion**

### 294 *5.1 Baldwin Lake's Environmental Change from 125 – 10 ka*

295 The basal luminescence age results at 2700 cm depth, with potential dates of  $136 \pm 10$  ka ( $50^\circ\text{C}$   
296 IRSL signal) or  $124 \pm 8$  ka ( $225^\circ\text{C}$  IRSL signal; Table 1), suggested that deposition of the  
297 BDL12 sequence began during MIS 5e. This facies was largely comprised of dense, coarse,  
298 massive sand. With  $<1\%$  fine grains, we interpreted these basal sediments to be well-winnowed,  
299 and deposited under high-energy conditions. Fluvial and colluvial processes likely dominated  
300 erosion and transport in the alpine valley at this time, with the Baldwin Basin possibly connected  
301 to adjacent Lower Bear Basin (Figure 1). The transition to finer-grained clayey silt was abrupt  
302 and interpreted as a hiatus, largely because IRSL-dated results from either side of the break have  
303 a difference of  $\geq 10$  kyr over 1.3 m of core. Rapid sedimentation from Sugarloaf Mountain,

304 including possible landslide events (e.g. the Sugarloaf Fan; Figure 1), may have aided closure of  
305 the basin, and the separation of the Baldwin and Lower Bear Lake basins (Leidy, 2006; Stout,  
306 1976).

307  
308 Trace elements that were key to the interpretation of MIS 5e conditions are reported in Table 2  
309 with approximate values. Sediment upsection of the basal sand possessed high Ti and Fe, and  
310 low carbonate and organic content (Table 2, Figure 4). This largely detrital, inorganic deposition  
311 suggests that Baldwin Lake remained deep, unproductive, and cool for the first half of MIS 5d  
312 during a summer insolation minimum at 116 ka. Ca, CaCO<sub>3</sub>, and organics later increased at 112  
313 ka while MS decreased, indicating the lake became warmer, shallower, and more productive.

314  
315 The period centered around MIS 5c was the basin's first productive phase from 109 – 96 ka, with  
316 organic values reaching >30% on two occasions between 106 – 103 ka, and BSi of ~11.3 mg/g.  
317 Productivity declined to minimal levels by 95 ka (Table 2, Figure 4a-b). During MIS 5b – 5a (95  
318 – 71 ka), productivity again increased and decreased, reaching >30% at 83 ka. Lowstand  
319 conditions occurred during MIS 5b, with high Ca, CaCO<sub>3</sub>, and Mn:Ti (Table 2, Figure 4).  
320 Abundant littoral mollusks *Lymnaea* and *Planorbella* spp. (Burch, 1982) indicate that the lake  
321 shoreline had reached the basin depocenter, where the core was taken. All Ca-based lowstand  
322 evidence quickly disappeared at 82 ka, and organics surged to 33% by 81.6 ka in the deeper  
323 water, before declining alongside summer insolation to reach ~1% at 73 ka.

324  
325 During MIS 4 and 3, lower amplitude oscillations in summer insolation apparently yielded a  
326 long-term state of lake productivity, perhaps because seasonal insolation was less variable.

327 Organics increased from the onset of MIS 4 (71 ka), and then maintained moderate values  
328 (average = 16.4%; Figure 4b). Early MIS 4 had relatively high levels of Ca, CaCO<sub>3</sub>, and Mn:Ti  
329 (Table 2, Figure 4g-i) that declined over the ensuing ~5-6 kyr. These lower values persisted until  
330 the end of MIS 2, suggesting lake stratification, and infrequent ventilation. Meanwhile, biologic  
331 sedimentation increased (average bulk organics =18.8%) and underwent millennial-scale  
332 fluctuations, where bulk organic values ranged between 10 – 28%.

333

334 Periods of subtle laminae occurred during the first half of MIS 3 (57 – 46 ka), and are described  
335 in greater detail for core BLDC04-2 (Kirby et al., 2006). While laminated and non-laminated  
336 sediment may indicate lake water level shifts (Retelle and Child, 1996), we do not find support  
337 for the alternating perennial-to-playa conditions during MIS 3 proposed by Blazevic et al.  
338 (2009). The sediments and their chemistry are not consistent with playa conditions, best  
339 characterized by the elemental “signature” of high Ca, CaCO<sub>3</sub>, and Mn:Ti that marked Baldwin  
340 Lake’s desiccation at the onset of the Holocene (Figure 4g-i). The abovementioned low  
341 concentrations of these elements persisted during MIS 3, along with low MS (Table 2, Figure  
342 4f), suggesting a lack of significant bottom ventilation events. These conditions lasted for most  
343 of MIS 4 and the duration of MIS 3, at least 35 kyr. This period of greater effective moisture in  
344 the SBM has also been noted in other parts of the Transverse Ranges (Santa Barbara Basin;  
345 Heusser, 1998), Valley Wells in the Mojave Desert (Pigati et al., 2011), and in the Great Basin  
346 (Maher et al., 2014).

347

348 Organic matter concentrations declined during the lower insolation and colder temperatures of  
349 MIS 2, after a final peak at 27.7 ka. Sedimentation slowed significantly and was largely detrital,



350 with Fe and Ti increasing into the Last Glacial Maximum (LGM, 26 – 19 ka; Figure 4d-e). BSi  
351 decreased to ~5 mg/g by the end of MIS 2, but moderate values (~5 – 10 mg/g) until that time  
352 (Table 2, Figure 4) suggest continued productivity, despite the cold conditions and reduced light  
353 availability in the early part of this glacial. Glacial conditions can produce a sparsely-vegetated  
354 landscape and enhanced runoff capable of maintaining relatively high diatom productivity  
355 (Ampel et al., 2008), and the high Fe and Ti values suggest a similar response in the Baldwin  
356 Lake basin. The highest MS excursion in the core occurred at 27 – 25.5 ka; aside from oxidation  
357 of the core since its collection, there are no other unique sedimentary structures, nor shifts in  
358 other proxy data, that correspond to this excursion. One possible interpretation for this high MS  
359 peak was a decrease in reducing conditions, which would preserve the magnetic signal (Dearing,  
360 1999).

361  
362 Shallow-water indicators Ca, CaCO<sub>3</sub>, and Mn:Ti increased suddenly around 12 ka, after which  
363 time Baldwin Lake likely transitioned to an intermittent, playa surface as summer insolation rose  
364 from 23 – 11 ka. Frequent dry episodes prevented further preservation of biologic material.

365 While the Holocene is a notable omission in BDL12, a Holocene-age paleorecord from  
366 neighboring Lower Bear Lake (Figure 1) has provided insight into SBM climate since 9.3 ka  
367 (Kirby et al., 2012).

368

## 369 5.2 Important Climatic Drivers in Southern California

### 370 5.2.1 Orbital-Scale Radiative Forcing

371 California pollen sites that date to MIS 5e, including the Santa Barbara Basin (ODP 893;  
372 Heusser, 1998), ODP 1018 (Lyle et al., 2010), and Owens Lake (Woolfenden, 2003) have shown

373 orbitally-induced landscape change. The influence of boreal summer insolation, largely credited  
374 with driving continental ice sheet mass, was a primary driver of change at interior Great Basin  
375 speleothem sites including the Leviathan, Pinnacle, and Lehman Caves (Lachniet et al., 2014),  
376 and Devil’s Hole (Moseley et al., 2016). The high-amplitude shifts detected in organic matter  
377 during MIS 5 in BDL12 suggest that organic deposition was a primary response to local summer  
378 insolation, a relationship first proposed for the shorter Baldwin Lake sequence (Kirby et al.,  
379 2006).

380

381 Globally, MIS 4 conditions were milder compared to other glacials, including in the North  
382 American West and Sierra Nevada (Brook et al., 2006; Forester et al., 2005; Jiménez-Moreno et  
383 al., 2010; Phillips et al., 1996; Rood et al., 2011). At Baldwin Lake, summer insolation minima  
384 likely drove cold conditions that were short-lived, as the primary productivity increased and  
385 recovered within a few kyr of MIS 4 onset. During MIS 3, both winter and summer insolation  
386 were at their least variable in the record, reducing local seasonality (Figure 5c). Summer  
387 insolation varied between 481 – 509 W/m<sup>2</sup>, while winter insolation was relatively static (Figure  
388 5c, Table 2). This may have allowed the lake to remain ice-free, and for primary productivity to  
389 continue, for longer durations each year compared to other MISs. During MIS 2, summer  
390 insolation declined to only 471 W/m<sup>2</sup> (23 ka) compared to 465 W/m<sup>2</sup> in MIS 4, but winter  
391 insolation was slightly lower (234 W/m<sup>2</sup> vs. 239 W/m<sup>2</sup>). Summer insolation reached 515 W/m<sup>2</sup> at  
392 11 ka, the first time since 81 ka that radiation reached such levels. Proxy data (e.g. trace element  
393 Ca and CaCO<sub>3</sub> maxima) suggest that the lake was shallow and warm at the onset of the  
394 Holocene, a different set of conditions compared to earlier, equivalent summer insolation  
395 maxima during MIS 5 ( $\geq 510$  W/m<sup>2</sup>). Enhanced evaporation and shifting precipitation are

396 possible causes for the end of perennial conditions at Baldwin Lake, as well as the infilling of the  
397 basin (~16 m of deposition between 81 and 11 ka). After 11 ka, sediments that are massive, high-  
398 carbonate, and degraded suggest that intermittent deposition likely continued, with periods of  
399 desiccation that compromised sediment chemical and biologic preservation. Other sites in arid  
400 and semiarid California exhibited similar transitions from relatively wet towards intermittent or  
401 dry conditions at the Pleistocene-to-Holocene transition, including Owens Lake (Bacon et al.,  
402 2006) and Lake Manly/Death Valley (Li et al., 1996).

403

#### 404 5.2.2 Millennial-Scale Forcing during MIS 3

405 We have shown that major productivity shifts in Baldwin Lake likely occurred at the slow pace  
406 of orbital variation, though these changes were not without shorter-order minima and maxima,  
407 particularly during MIS 3. What rapid processes account for such change? Kirby et al. (2006)  
408 proposed these were wet events corresponding to North Atlantic interstadials, or Dansgaard-  
409 Oeschger (D-O) events. D-O events were North Atlantic millennial-scale temperature  
410 oscillations that occur between 120 and 10 ka, first recognized in  $\delta^{18}\text{O}$  data from the Greenland  
411 ice cores (Dansgaard et al., 1993). Interstadial-stadial couplets typically had a rapid onset,  
412 followed by gradual cooling (Grootes et al., 1993; Johnsen et al., 1992). Freshwater discharge to  
413 the North Atlantic increased during interstadials, likely reducing deep water formation and  
414 impacting Atlantic Meridional Overturning Circulation. Rapid transmission of a dynamic climate  
415 signal to the globe within decades was the net result (Elliot et al., 2002; Gottschalk et al., 2015),  
416 though regional response, duration and precise timing differed from the Greenland chronology.

417

418 D-O events propagated to the North Pacific (Lund and Mix, 1998), and Hendy and Kennett  
419 (2000a) have documented D-O events in the Santa Barbara Basin (SBB) with oxygen isotopes,  
420 and shifts in benthic foraminifera assemblages that support warmer SSTs during interstadials  
421 (Figure 5a, 5b). Behl and Kennett (1996) noted laminations driven by anoxia during D-O  
422 interstadials. Thus, the SBB response during MIS 3 interstadials was enhanced marine  
423 temperatures, driven by increased influx of subtropical waters and weaker California Current  
424 (Hendy and Kennett, 2000a). In Owens Lake, total organic carbon apparently increased in  
425 tandem with D-O interstadials, though ascribing specific events to these %TOC fluctuations is  
426 largely speculative, due to chronological uncertainties (Benson et al., 2003, 2002).

427

428 We found a similar response in Baldwin Lake's total organic matter. Within the limits of dating  
429 uncertainties, there was apparent synchronicity between terrestrial BDL12, marine SBB, and  
430 NGRIP  $\delta^{18}\text{O}$  in the timing, duration, and relative amplitude of D-O interstadials. We suggest D-  
431 O event numbers for BDL12 (Figure 5c) after conventions of Rasmussen et al. (2014). Core gaps  
432 and noisy organic data occurred between 60 – 52 ka, however, and winter insolation prior to 50  
433 ka may have dampened the amplitude of potential D-O interstadials (Figure 5c). Rasmussen et al.  
434 (2014) confirm that the North Atlantic response from 59 – 54 ka was a complex transition  
435 between global climatic states, and complex sub-intervals during D-O interstadials from this  
436 interval have been identified since initial identification and numbering. Thus, D-O interstadials  
437 16-17 were not assigned to specific organic peaks in BDL12, but likely occurred over a 3-5 kyr  
438 interval of high-amplitude, rapid changes (Figure 5c). Despite these caveats, millennial-scale  
439 fluctuations in Baldwin Lake organic deposition suggest that North Atlantic MIS 3 and MIS 2

440 perturbations were strong enough to influence Southern California climate during a period of  
441 intermediate insolation.

442

443 5.3 Pacific- and North Atlantic-induced events in California, the Great Basin, and Southwest

444 We examined other paleoclimate sites in California, the Great Basin, and Southwest (Figure 6)

445 for their response to rapid change, and asked 1) which events are coeval to environmental

446 changes in the SBM, 2) was there a temperature and/or hydrological response at each site, and 3)

447 is there a coherent geographic pattern of response? We focused largely on 85 – 20 ka, the period

448 with the greatest number of comparative sites to BDL12, mapped in Figures 6 and 7 with the

449 ecoregions of Bailey (2009).

450

451 MIS 5a events in BDL12 included lowstands at 87 and 82 ka. The 82 ka event in particular was

452 coeval with other evidence of warm conditions throughout the West, including a marine

453 highstand along the California and Southern Oregon coasts 84 – 76 ka (Muhs et al., 2012).

454 Devil's Hole experienced a maximum in  $\delta^{18}\text{O}$  isotopic values (82.5  $\pm$ 0.7 ka; Moseley et al.,

455 2016), and the onset of warm SSTs at ODP 1017 occurred 82 ka (Seki et al., 2002). Baldwin

456 Lake rapidly transgressed after 82 ka over the course of 0.6 – 0.7 kyr, suggesting a sudden

457 change in either basin deposition, or moisture regime.

458

459 Widespread climatic change next happened at terrestrial sites during the 3 kyr period spanning

460 Heinrich Event 6 (H6, 60  $\pm$  5 ka; Hemming, 2004) and the transition to MIS 3 (57 ka). Several

461 terrestrial sites underwent hydrologic shifts. Lake Manley in Death Valley transitioned from

462 mudflat to more arid saltpan ~59 – 57 ka (Forester et al., 2005). Runoff to Lake Babicora,

463 located at the southernmost extent of the region shown (Figure 6), also reduced 58 ka (Roy et al.,  
464 2013). In contrast, other sites in Southern California became wet, including Baldwin Lake's  
465 perennial lake phase throughout MIS 3, and the onset of groundwater flow in Valley Wells 60 ka  
466 (Figure 6; Pigati et al., 2011). West of the Sierra Nevada, peak moisture included a wetter phase  
467 from  $61.7 \pm 0.5$  to  $59.8 \pm 0.6$  ka at McLean's Cave, with a return to relatively dry conditions  
468 afterwards (Oster et al., 2014). This demonstrated the site's sensitivity to North Atlantic  
469 changes: Heinrich 6 ( $60 \pm 5$  ka; Hemming, 2004) coincided with wet conditions, and D-O  
470 interstadials 15–18 were arid phases in the Sierra Nevada foothills (Oster et al., 2014).  
471 Meanwhile, ice-rafted debris from increased freshwater runoff reached a maximum 59 – 58 ka at  
472 Mono Lake east of the Sierra Nevada (Zimmerman et al., 2011).

473  
474 Thus, terrestrial hydrologic change is not uniform throughout California at the MIS 4/3  
475 transition, though wetter sites tended to cluster in the southern sector of the Mojave Desert and  
476 the SBM. Offshore sites responded consistently with enhanced SSTs initiating close to the MIS  
477 4/3 transition at sites 1014, 1017, and 1012, but hydrologic change was difficult to determine  
478 from available records and proxy data (Hendy et al., 2004; Hendy and Kennett, 2000b; Herbert et  
479 al., 2001; Seki et al., 2002). High resolution BSi data from ODP 1018 showed increasing SSTs  
480 61 ka, and these data provide insight to other processes and moisture at the Northern California  
481 site: enhanced SSTs were accompanied with greater productivity, suppressed upwelling, and  
482 aridity that lasted 8-10 kyr (Lyle et al., 2010).

483  
484 More sites span MIS 3, including recently-developed records that depend upon groundwater  
485 infiltration (e.g. speleothem records, soil precipitates, and groundwater/desert wetland deposits).

486 We synthesize the sensitivity of paleoclimatic records to D-O interstadials, noting if the response  
487 was cold, warm, wet or dry (Figure 7). The investigators' original climatic interpretation for D-O  
488 interstadial response were used in this map. Uncertainty in dating methods can be several  
489 millennia at sites of MIS 3 age, a recognized problem in trying to detect events that last, on  
490 average, ~1.48 kyr (Benson et al., 2003; Denniston et al., 2007; Zimmerman et al., 2011). Still,  
491 mapping current knowledge of D-O interstadial response in a large sector of the North American  
492 West did show emergent patterns, and may provide a framework for future hypothesis-testing at  
493 regional paleoclimate sites.

494  
495 High-resolution marine records ODP 1017 and 1014 responded to D-O interstadials with warmer  
496 SSTs (Hendy and Kennett, 2000b; Hendy and Pedersen, 2005; Pak et al., 2012; Pospelova et al.,  
497 2015; Seki et al., 2002). Heusser (1998) detected millennial-scale increases in ODP 893 oak  
498 pollen, a dry-adapted taxa, that corresponded to D-O interstadials. Enhanced aridity was the  
499 norm during D-O interstadials at terrestrial sites, including Southwestern speleothem records  
500 Fort Stanton, Carlsbad Cavern, and Cave of the Bells (Asmerom et al., 2010; Brook et al., 2006;  
501 Wagner et al., 2010). In the tropical-temperate desert south of the Great Basin, sites demonstrate  
502 a potential sensitivity to D-O interstadials quite late, with arid fluctuations that start at 35 ka (e.g.  
503 Searles Lake, Lin et al., 1998; Las Vegas Valley, Springer et al., 2015). Sites that experienced  
504 overall greater effective moisture throughout MIS 3, but did not exhibit consistent millennial-  
505 scale variability, include Valley Wells (Pigati et al., 2011), the San Pedro Valley (Pigati et al.,  
506 2009). Records in Mexico began to show a sensitivity to D-O events by mid-MIS 3 (42 – 40 ka),  
507 with warmer SSTs in the Gulf of California (Price et al., 2013) and enhanced moisture at Lake  
508 Babicora (Roy et al., 2013).

509

510 The Great Basin response to D-O interstadials varied geographically, with enhanced moisture at  
511 its northern and western margins, and no apparent response towards the interior (Figure 7).  
512 Millennial-scale oscillations were absent from Lehman, Leviathan, and Pinnacle speleothem  
513 records (Lachniet et al., 2014), and groundwater precipitates (Franklin, Newark Valley, Diamond  
514 Valley, Barstow, and Yucca Mountain, Figure 6-7; Maher et al., 2014). Higher lake levels during  
515 interstadials occur at Mono, Pyramid, and Owens Lakes to the east of the Sierra Nevada (Benson  
516 et al., 2003). The northeastern Great Basin underwent saline and hypersaline oscillations in the  
517 Great Salt Lake during MIS 3 (Balch et al., 2005), and Benson et al. (2011) interpreted higher  
518 lake levels and wet D-O interstadials for this sector of the Lake Bonneville Basin. This wet  
519 response at the margins of the Great Basin may be due to nearby glaciers and the Laurentide Ice  
520 Sheet, a potential source of meltwater during warm excursions.

521

522 In the SBM, Kirby et al. (2006) previously hypothesized that D-O interstadials were wet  
523 episodes based upon laminated deposits in deep water conditions, but laminated horizons  
524 observed in BDL12 did not reliably match the organic excursions proposed as the D-O  
525 interstadials. Directly-dated relict shorelines at paleolake Manix to the north, part of the Mojave  
526 River watershed with its headwaters in the SBM, showed that D-O stadials were unusually wet  
527 for the region (Reheis et al., 2015). Yet with no supporting evidence in our current dataset that  
528 D-O interstadials enhanced moisture in alpine Southern California, the hydrologic response at  
529 Baldwin Lake remains ambiguous. North of the SBM in the Mojave Desert, and eastward  
530 towards the Southwest, the geographic pattern of response to D-O interstadials was enhanced  
531 aridity (Figure 7).



532

533 Reduced insolation, reduced evaporation, and generally wet conditions prevailed in Southern  
534 California and the Southwest at the MIS 3/2 transition at 29 ka, with some centennial- to  
535 millennial arid events. Groundwater infiltration prevailed in the Great Basin until 24 ka (Maher  
536 et al., 2014), while a highstand persisted at Owens Lake (Bacon et al., 2006) and Lake Manly (Li  
537 et al., 1996). Cave of the Bells (Wagner et al., 2010) and the San Pedro Valley sites of Pigati et  
538 al. (2009) were wet from 25 – 20 ka. An arid episode just prior to the LGM was evident at  
539 several of these sites, best documented with a well-dated, highly-resolved pollen study at Lake  
540 Elsinore that showed a ~2 kyr drought from 27.5 – 25.5 ka (Heusser et al., 2015). Other arid  
541 episodes that interrupted otherwise wet conditions include reversals at Owens Lake 25-24 ka  
542 (Bacon et al., 2006), Pyramid Lake at 29 ka (Benson et al., 2013), and a pair of lakes on the  
543 Colorado Plateau at 24.5 – 24 ka (Hay and Walker Lakes; Anderson et al., 2000). The high  
544 magnetic susceptibility excursion at Baldwin Lake was contemporaneous with the Lake Elsinore  
545 drought, and could have been caused by rapid sediment burial or lake mixing (Dearing, 1999).

546

547 An influx of Pacific moisture arrived in Southern California by 22 ka (Oster et al., 2015). Lake  
548 highstand and basin spillover events towards the east are events often mentioned as part of Big  
549 Bear Valley's Ice Age history (Krantz, 1983; Leidy, 2006; Stout, 1976), but the evidence has not  
550 been directly dated. Glaciation occurred for ~5 kyr on San Gorgonio, the highest-elevation peak  
551 in the SBM, depositing a series of moraines 20 – 16 ka and 16 – 15 ka (Owen et al., 2003). The  
552 early MIS 2 drought at Lake Elsinore 27.5 – 25.5 ka, and subsequent moisture influx ~22 ka,  
553 suggest that Southern California had a complex and dynamic hydrologic history during the Last  
554 Ice Age, with changes occurring on millennial, and perhaps submillennial, scales. Further study

555 with tighter-resolution proxy analyses are necessary to better resolve these events in space and  
556 time.

557

## 558 **6. Conclusions**

559 Physical and geochemical proxy analyses on Baldwin Lake suggest that Southern California  
560 climate change was sensitive to orbitally-induced radiation over the past 125 ka, particularly in  
561 material recovered from MIS 5. Variations in local summer insolation during MIS 5e-5a (125 –  
562 71 ka) were large, ranging 448 – 533 W/m<sup>2</sup>, and likely the primary cause of high-amplitude  
563 shifts in lake productivity. Summer insolation was less pronounced during MIS 4 – 3 (71 – 29  
564 ka; 465 – 510 W/m<sup>2</sup>), while winter insolation was relatively stable. During the combined effects  
565 of intermediate radiation and reduced seasonal variability, portions of the North American West,  
566 particularly Southern California, experienced 1) greater effective moisture throughout MIS 3,  
567 and 2) sensitivity to North Atlantic forcing, namely Dansgaard-Oeschger (D-O) interstadial  
568 events.

569

570 The influence of D-O interstadials on California, the Great Basin, and U.S. Southwest during  
571 MIS 3 -2 produced a geographically varied response. In alpine Southern California, productivity  
572 increases in the Baldwin Lake core were the apparent responses to D-O interstadials. While we  
573 have no direct measure of hydrologic change during these interstadials in the present study,  
574 enhanced aridity was a consistent response at sensitive sites in the surrounding Mojave Desert,  
575 and eastward into the Southwest. Sites on the western and northeastern margins of the Great  
576 Basin were wet during D-O interstadials, and no consistent millennial-scale events have been  
577 detected at Great Basin interior sites during MIS 3. MIS 2 brought depressed insolation and cold,

578 glacial conditions with variable moisture. While summer insolation did not quite reach MIS 5  
579 maxima ( $\sim 530\text{-}540\text{ W/m}^2$ ) at the MIS 2/1 transition, climate was warm and/or dry enough to  
580 cause Southern California lakes to transition to intermittent, or playa, states. Baldwin Lake has  
581 been an intermittent lake since  $\sim 12\text{ ka}$ .

582

583 This work highlights the sensitivity of Southern California's climate to radiative and oceanic  
584 forcing, and the need to better understand how the ocean-atmospheric system reorganizes itself  
585 to transmit such changes. It is also clear that during past climate states, radiative and oceanic  
586 forcing produced hydrologic responses that varied geographically. Improved understanding of  
587 the nature and drivers of this variability is an urgent need at present, as recent studies (e.g. Cayan  
588 et al., 2010; Diffenbaugh et al., 2015; Overpeck and Udall, 2010) forecast an increasingly warm  
589 and arid Southern California and Southwest for the rest of the 21<sup>st</sup> century. Enhanced  
590 temperature and aridity will certainly produce stresses on the region's population and  
591 ecosystems.

592

### 593 **Acknowledgments**

594 We are grateful for the financial support provided by the UCLA Institute of the Environment and  
595 Sustainability Presidential Fund, UCLA Graduate Division, Limnological Research Center,  
596 Geological Society of America, UCLA Dept. of Geography John Muir Memorial Endowment,  
597 Society of Woman Geographers, and the Department of the Interior Southwest Climate Science  
598 Center. Fieldwork and core recovery were greatly assisted by Katie Nelson, Scott Eliason, and  
599 Gina Griffith of the San Bernardino National Forest; Larry Winslow of Big Bear, CA; and Gregg  
600 Drilling, L.L.C. KCG especially thanks Wendy Barrera for leading IRSL subsampling and

601 preparation at the UCLA Luminescence Laboratory, assistance from Jessica Rodysill and  
602 Kristina Brady while visiting the Limnological Research Center at the University of Minnesota,  
603 and Katherine Whitacre at Northern Arizona University’s Amino Acid Geochronology Lab. We  
604 thank several students for their assistance in the field and lab, including Lauren Brown, April  
605 Chaney, Elaine Chang, Christine Hiner, Tamryn Kong, Alec Lautanen, Jennifer Leidelmeijer,  
606 Setareh Nejat, Alex Pakalniskis, Sargam Saraf, Nicole Tachiki, Marcus Thomson, Alice Wong,  
607 Alex Woodward and Renée Yun. The thorough and thoughtful comments of two anonymous  
608 reviewers greatly improved the paper, and are much appreciated. Candid conversation and  
609 feedback from many of the investigators cited, too numerous to name here, have also improved  
610 our discussion of long-term climate change in the North American West.

611

612

613

614 **7. References**

- 615 Ampel, L., Wohlfarth, B., Risberg, J., Veres, D., 2008. Paleolimnological response to millennial  
616 and centennial scale climate variability during MIS 3 and 2 as suggested by the diatom  
617 record in Les Echets, France. *Quat. Sci. Rev.* 27, 1493–1504.  
618 doi:10.1016/j.quascirev.2008.04.014
- 619 Anderson, R.S., Betancourt, J.L., Mead, J.I., Hevly, R.H., Adam, D.P., 2000. Middle- and late-  
620 Wisconsin paleobotanic and paleoclimatic records from the southern Colorado Plateau,  
621 USA. *Palaeogeogr. Palaeoclimatol. Palaeoecol.* 155, 31–57. doi:10.1016/S0031-  
622 0182(99)00093-0
- 623 Asmerom, Y., Polyak, V.J., Burns, S.J., 2010. Variable winter moisture in the southwestern  
624 United States linked to rapid glacial climate shifts. *Nat. Geosci.* 3, 114–117.  
625 doi:10.1038/ngeo754
- 626 Bacon, S.N., Burke, R.M., Pezzopane, S.K., Jayko, A.S., 2006. Last glacial maximum and  
627 Holocene lake levels of Owens Lake, eastern California, USA. *Quat. Sci. Rev.* 25, 1264–  
628 1282. doi:10.1016/j.quascirev.2005.10.014
- 629 Bailey, R.G., 2009. *Ecosystem geography: from ecoregions to sites*, 2nd ed. ed. Springer, New  
630 York.
- 631 Balch, D.P., Cohen, A.S., Schnurrenberger, D.W., Haskell, B.J., Valero Garces, B.L., Beck,  
632 J.W., Cheng, H., Edwards, R.L., 2005. Ecosystem and paleohydrological response to  
633 Quaternary climate change in the Bonneville Basin, Utah. *Palaeogeogr. Palaeoclimatol.*  
634 *Palaeoecol.* 221, 99–122. doi:10.1016/j.palaeo.2005.01.013
- 635 Barron, J.A., Heusser, L., Herbert, T., Lyle, M., 2003. High-resolution climatic evolution of  
636 coastal northern California during the past 16,000 years. *Paleoceanography* 18, n/a-n/a.  
637 doi:10.1029/2002PA000768
- 638 Behl, R.J., Kennett, J.P., 1996. Brief interstadial events in the Santa Barbara basin, NE Pacific,  
639 during the past 60 kyr. *Nature* 379, 243–246. doi:10.1038/379243a0
- 640 Benson, L., Lund, S., Negrini, R., Linsley, B., Zic, M., 2003. Response of North American Great  
641 Basin Lakes to Dansgaard–Oeschger oscillations. *Quat. Sci. Rev.* 22, 2239–2251.  
642 doi:10.1016/S0277-3791(03)00210-5
- 643 Benson, L.V., Kashgarian, M., Rye, R.O., Lund, S.P., Paillet, F., Smoot, J.P., Kester, C.,  
644 Mensing, S.A., Meko, D.M., Lindström, S., 2002. Holocene Multidecadal and  
645 Multicentennial Droughts Affecting Northern California and Nevada. *Quat. Sci. Rev.* 21,  
646 659–682.
- 647 Benson, L.V., Lund, S.P., Smoot, J.P., Rhode, D.E., Spencer, R.J., Verosub, K.L., Louderback,  
648 L.A., Johnson, C.A., Rye, R.O., Negrini, R.M., 2011. The rise and fall of Lake  
649 Bonneville between 45 and 10.5 ka. *Quat. Int.* 235, 57–69.  
650 doi:10.1016/j.quaint.2010.12.014
- 651 Benson, L.V., Smoot, J.P., Lund, S.P., Mensing, S.A., Foit, F.F., Rye, R.O., 2013. Insights from  
652 a synthesis of old and new climate-proxy data from the Pyramid and Winnemucca lake

- 653 basins for the period 48 to 11.5 cal ka. *Quat. Int.* 310, 62–82.  
 654 doi:10.1016/j.quaint.2012.02.040
- 655 Big Bear Lake TMDL Task Force [WWW Document], 2012. URL  
 656 <http://www.sawpa.org/collaboration/past-projects/big-bear-lake-tmdl-taskforce/> (accessed  
 657 6.18.14).
- 658 Bird, B.W., Kirby, M.E., 2006. An Alpine Lacustrine Record of Early Holocene North American  
 659 Monsoon Dynamics from Dry Lake, Southern California (USA). *J. Paleolimnol.* 35, 179–  
 660 192. doi:10.1007/s10933-005-8514-3
- 661 Blaauw, M., Christen, J.A., 2011. Flexible Paleoclimate Age-Depth Models Using an  
 662 Autoregressive Gamma Process. *Bayesian Anal.* 6, 457–474. doi:10.1214/11-BA618
- 663 Blass, A., Bigler, C., Grosjean, M., Sturm, M., 2007. Decadal-scale autumn temperature  
 664 reconstruction back to AD 1580 inferred from the varved sediments of Lake Silvaplana  
 665 (southeastern Swiss Alps). *Quat. Res.* 68, 184–195. doi:10.1016/j.yqres.2007.05.004
- 666 Blazevic, M.A., Kirby, M.E., Woods, A.D., Browne, B.L., Bowman, D.D., 2009. A sedimentary  
 667 facies model for glacial-age sediments in Baldwin Lake, Southern California. *Sediment.*  
 668 *Geol.* 219, 151–168. doi:10.1016/j.sedgeo.2009.05.003
- 669 Brook, G.A., Ellwood, B.B., Railsback, L.B., Cowart, J.B., 2006. A 164 ka record of  
 670 environmental change in the American Southwest from a Carlsbad Cavern speleothem.  
 671 *Palaeogeogr. Palaeoclimatol. Palaeoecol.* 237, 483–507.  
 672 doi:10.1016/j.palaeo.2006.01.001
- 673 Brunelle, A., Anderson, R.S., 2003. Sedimentary charcoal as an indicator of late-Holocene  
 674 drought in the Sierra Nevada, California, and its relevance to the future. *The Holocene*  
 675 13, 21–28. doi:10.1191/0959683603hl591rp
- 676 Burch, J.B., 1982. Freshwater snails (Mollusca: Gastropoda) of North America (No. EPA-600/3-  
 677 82-026). United States Environmental Protection Agency.
- 678 Buylaert, J.P., Murray, A.S., Thomsen, K.J., Jain, M., 2009. Testing the potential of an elevated  
 679 temperature IRSL signal from K-feldspar. *Radiat. Meas.* 44, 560–565.  
 680 doi:10.1016/j.radmeas.2009.02.007
- 681 Cacho, I., Grimalt, J.O., Pelejero, C., Canals, M., Sierro, F.J., Flores, J.A., Shackleton, N., 1999.  
 682 Dansgaard-Oeschger and Heinrich event imprints in Alboran Sea paleotemperatures.  
 683 *Paleoceanography* 14, 698–705. doi:10.1029/1999PA900044
- 684 Cayan, D.R., Das, T., Pierce, D.W., Barnett, T.P., Tyree, M., Gershunov, A., 2010. Future  
 685 dryness in the southwest US and the hydrology of the early 21st century drought. *Proc.*  
 686 *Natl. Acad. Sci.* 107, 21271–21276. doi:10.1073/pnas.0912391107
- 687 Cayan, D.R., Peterson, D.H., 1989. The influence of North Pacific atmospheric circulation on  
 688 streamflow in the west., in: *Aspects of Climate Variability in the Pacific and the Western*  
 689 *Americas*. American Geophysical Union, pp. 375–397.
- 690 Climate - Southern California Average Annual Precipitation [WWW Document], n.d. . *Clim. -*  
 691 *South. Calif. Aver. Annu. Precip.* URL [http://www.wrh.noaa.gov/sgx/climate/pcpn-](http://www.wrh.noaa.gov/sgx/climate/pcpn-avg.php?wfo=sgx)  
 692 [avg.php?wfo=sgx](http://www.wrh.noaa.gov/sgx/climate/pcpn-avg.php?wfo=sgx)

- 693 Colman, S.M., Peck, J.A., Karabanov, E.B., Carter, S.J., Bradbury, J.P., King, J.W., Williams,  
694 D.F., 1995. Continental climate response to orbital forcing from biogenic silica records in  
695 Lake Baikal. *Nature* 378, 769–771. doi:10.1038/378769a0
- 696 Conley, D.J., Schelske, C.L., 2002. Biogenic Silica, in: Smol, J.P., Birks, H.J.B., Last, W.M.,  
697 Bradley, R.S., Alverson, K. (Eds.), *Tracking Environmental Change Using Lake*  
698 *Sediments*. Kluwer Academic Publishers, Dordrecht, pp. 281–293.
- 699 Dansgaard, W., Johnsen, S.J., Clausen, H.B., Dahl-Jensen, D., Gundestrup, N.S., Hammer, C.U.,  
700 Hvidberg, C.S., Steffensen, N.S., Scejnbjörnsdottir, A.E., Jouzel, J., Bond, G., 1993.  
701 Climate instability during the last interglacial period recorded in the GRIP ice core.  
702 *Nature* 364, 203–207. doi:10.1038/364203a0
- 703 Dean, W.E., 1974. Determination of Carbonate and Organic Matter in Calcareous Sediments and  
704 Sedimentary Rocks by Loss on Ignition: Comparison With Other Methods. *SEPM J.*  
705 *Sediment. Res.* Vol. 44. doi:10.1306/74D729D2-2B21-11D7-8648000102C1865D
- 706 Dearing, J., 1999. *Environmental Magnetic Susceptibility: Using the Bartington MS2 System*,  
707 2nd ed. Chi Publishing, Kenilworth, England.
- 708 Denniston, R.F., Asmerom, Y., Polyak, V., Dorale, J.A., Carpenter, S.J., Trodick, C., Hoye, B.,  
709 González, L.A., 2007. Synchronous millennial-scale climatic changes in the Great Basin  
710 and the North Atlantic during the last interglacial. *Geology* 35, 619.  
711 doi:10.1130/G23445A.1
- 712 Dibblee, T.W., 1964. Geological map of the San Gorgonio Mountain Quadrangle, San  
713 Bernardino and Riverside Counties, California. *Miscellaneous Geologic Investigations*.
- 714 Diffenbaugh, N.S., Swain, D.L., Touma, D., 2015. Anthropogenic warming has increased  
715 drought risk in California. *Proc. Natl. Acad. Sci.* 112, 3931–3936.  
716 doi:10.1073/pnas.1422385112
- 717 Elliot, M., Labeyrie, L., Duplessy, J.-C., 2002. Changes in North Atlantic deep-water formation  
718 associated with the Dansgaard–Oeschger temperature oscillations (60–10ka). *Quat. Sci.*  
719 *Rev.* 21, 1153–1165. doi:10.1016/S0277-3791(01)00137-8
- 720 Flint, L.E., Martin, P., 2012. *Geohydrology of Big Bear Valley, California: Phase 1—Geologic*  
721 *Framework, Recharge, and Preliminary Assessment of the Source and Age of*  
722 *Groundwater (Scientific Investigations No. 2012–5100)*. U. S. Geological Survey.
- 723 Forester, R.M., Lowenstein, T.K., Spencer, R.J., 2005. An ostracode based paleolimnologic and  
724 paleohydrologic history of Death Valley: 200 to 0 ka. *Geol. Soc. Am. Bull.* 117, 1379.  
725 doi:10.1130/B25637.1
- 726 Garcia, A.L., Knott, J.R., Mahan, S.A., Bright, J., 2014. Geochronology and paleoenvironment  
727 of pluvial Harper Lake, Mojave Desert, California, USA. *Quat. Res.* 81, 305–317.  
728 doi:10.1016/j.yqres.2013.10.008
- 729 Georgescu, M., Moustauoui, M., Mahalov, A., Dudhia, J., 2012. Summer-time climate impacts of  
730 projected megapolitan expansion in Arizona. *Nat. Clim. Change* 3, 37–41.  
731 doi:10.1038/nclimate1656
- 732 Goring, S., Williams, J.E., Blois, J.L., Jackson, S.T., Paciorek, C.J., Booth, R.K., Marlon, J.R.,  
733 Blaauw, M., Christen, J.A., 2012. Deposition times in the northeastern United States

- 734 during the Holocene: establishing valid priors for Bayesian age models. *Quat. Sci. Rev.*  
735 48, 54–60.
- 736 Gottschalk, J., Skinner, L.C., Misra, S., Waelbroeck, C., Menviel, L., Timmermann, A., 2015.  
737 Abrupt changes in the southern extent of North Atlantic Deep Water during Dansgaard–  
738 Oeschger events. *Nat. Geosci.* 8, 950–954. doi:10.1038/ngeo2558
- 739 Groot, M.H.M., van der Plicht, J., Hooghiemstra, H., Lourens, L.J., Rowe, H.D., 2014. Age  
740 modelling for Pleistocene lake sediments: A comparison of methods from the Andean  
741 Fúquene Basin (Colombia) case study. *Quat. Geochronol.* 22, 144–154.  
742 doi:10.1016/j.quageo.2014.01.002
- 743 Grootes, P.M., Stuiver, M., White, J.W.C., Johnsen, S., Jouzel, J., 1993. Comparison of oxygen  
744 isotope records from the GISP2 and GRIP Greenland ice cores. *Nature* 366, 552–554.  
745 doi:10.1038/366552a0
- 746 Hahn, A., Kliem, P., Ohlendorf, C., Zolitschka, B., Rosén, P., 2013. Climate induced changes as  
747 registered in inorganic and organic sediment components from Laguna Potrok Aike  
748 (Argentina) during the past 51 ka. *Quat. Sci. Rev.* 71, 154–166.  
749 doi:10.1016/j.quascirev.2012.09.015
- 750 Heiri, O., Lotter, A.F., Lemcke, G., 2001. Loss on ignition as a method for estimating organic  
751 and carbonate content in sediments: reproducibility and comparability of results. *J.*  
752 *Paleolimnol.* 25, 101–110.
- 753 Hemming, S.R., 2004. Heinrich events: Massive late Pleistocene detritus layers of the North  
754 Atlantic and their global climate imprint. *Rev. Geophys.* 42. doi:10.1029/2003RG000128
- 755 Hendy, I.L., Kennett, J.P., 2000. Dansgaard-Oeschger Cycles and the California Current System:  
756 Planktonic foraminiferal response to rapid climate change in Santa Barbara Basin, Ocean  
757 Drilling Program Hole 893A. *Paleoceanography* 15, 30. doi:10.1029/1999PA000413
- 758 Hendy, I.L., Kennett, J.P., 2000. Stable isotope stratigraphy and paleoceanography of the last  
759 170 ky: Site 1014, Tanner Basin, California., in: *Proceedings of the Ocean Drilling*  
760 *Program, Scientific Results.* pp. 129–140.
- 761 Hendy, I.L., Pedersen, T.F., 2005. Is pore water oxygen content decoupled from productivity on  
762 the California Margin? Trace element results from Ocean Drilling Program Hole 1017E,  
763 San Lucia slope, California: PRODUCTIVITY-PORE WATER OXYGEN  
764 DECOUPLING. *Paleoceanography* 20, n/a-n/a. doi:10.1029/2004PA001123
- 765 Hendy, I.L., Pedersen, T.F., Kennett, J.P., Tada, R., 2004. Intermittent existence of a southern  
766 Californian upwelling cell during submillennial climate change of the last 60 kyr.  
767 *Paleoceanography* 19, n/a-n/a. doi:10.1029/2003PA000965
- 768 Herbert, T.D., Schuffert, J., Andreasen, D., Heusser, L.E., Lyle, M., Mix, A., Ravelo, A.C.,  
769 Stott, L.D., Herguera, J.C., 2001. Collapse of the California Current During Glacial  
770 Maxima Linked to Climate Change on Land. *Science* 293, 71–76.  
771 doi:10.1126/science.1059209
- 772 Heusser, L., 1998. Direct correlation of millennial-scale changes in western North American  
773 vegetation and climate with changes in the California Current System over the past ~60  
774 kyr. *Paleoceanography* 13, 252–262. doi:10.1029/98PA00670



- 775 Heusser, L.E., Basalm, W.L., 1977. Pollen Distribution in the Northeast Pacific Ocean. *Quat.*  
776 *Res.* 7, 45–62.
- 777 Heusser, L.E., Kirby, M.E., Nichols, J.E., 2015. Pollen-based evidence of extreme drought  
778 during the last Glacial (32.6–9.0 ka) in coastal southern California. *Quat. Sci. Rev.* 126,  
779 242–253. doi:10.1016/j.quascirev.2015.08.029
- 780 Hodell, D.A., Schelske, C.L., Fahnenstiel, G.L., Robbins, L.L., 1998. Biologically induced  
781 calcite and its isotopic composition in Lake Ontario. *Limnol. Oceanogr.* 43, 187–199.
- 782 Hooghiemstra, H., Lézine, A.-M., Leroy, S.A.G., Dupont, L., Marret, F., 2006. Late Quaternary  
783 palynology in marine sediments: A synthesis of the understanding of pollen distribution  
784 patterns in the NW African setting. *Quat. Int.* 148, 29–44.  
785 doi:10.1016/j.quaint.2005.11.005
- 786 Hu, F.S., Kaufman, D.S., Yoneji, S., Nelson, D., Shemesh, A., Huang, Y., Tian, J., Bond, G.,  
787 Clegg, B., Brown, T., 2003. Cyclic Variation and Solar Forcing of Holocene Climate in  
788 the Alaskan Subarctic. *Science* 301, 1890–1893. doi:10.1126/science.1088568
- 789 Imbrie, J., Hays, J.D., Martinson, D.G., McIntyre, A., Mix, A.C., Morley, J.J., Pisias, N., Prell,  
790 W.L., Shackleton, N.J., 1984. The orbital theory of Pleistocene climate: Support from a  
791 revised chronology of the marine  $\delta^{18}O$  record., in: *Ilankovitch and Climate:*  
792 *Understanding the Response to Astronomical Forcing.* p. 269.
- 793 Jiménez-Moreno, G., Anderson, R.S., Desprat, S., Grigg, L.D., Grimm, E.C., Heusser, L.E.,  
794 Jacobs, B.F., López-Martínez, C., Whitlock, C.L., Willard, D.A., 2010. Millennial-scale  
795 variability during the last glacial in vegetation records from North America. *Quat. Sci.*  
796 *Rev.* 29, 2865–2881. doi:10.1016/j.quascirev.2009.12.013
- 797 Johnsen, S.J., Clausen, H.B., Dansgaard, W., Fuhrer, K., Gundestrup, N., Hammer, C.U.,  
798 Iversen, P., Jouzel, J., Stauffer, B., steffensen, J.P., 1992. Irregular glacial interstadials  
799 recorded in a new Greenland ice core. *Nature* 359, 311–313. doi:10.1038/359311a0
- 800 Kaplan, M.R., Wolfe, A.P., Miller, G.H., 2002. Holocene Environmental Variability in Southern  
801 Greenland Inferred from Lake Sediments. *Quat. Res.* 58, 149–159.  
802 doi:10.1006/qres.2002.2352
- 803 Kirby, M.E., Feakins, S.J., Bonuso, N., Fantozzi, J.M., Hiner, C.A., 2013. Latest Pleistocene to  
804 Holocene hydroclimates from Lake Elsinore, California. *Quat. Sci. Rev.* 76, 1–15.  
805 doi:10.1016/j.quascirev.2013.05.023
- 806 Kirby, M.E., Knell, E.J., Anderson, W.T., Lachniet, M.S., Palermo, J., Eeg, H., Lucero, R.,  
807 Murrieta, R., Arevalo, A., Silveira, E., Hiner, C.A., 2015. Evidence for insolation and  
808 Pacific forcing of late glacial through Holocene climate in the Central Mojave Desert  
809 (Silver Lake, CA). *Quat. Res.* 84, 174–186. doi:10.1016/j.yqres.2015.07.003
- 810 Kirby, M.E., Lund, S.P., Anderson, M.A., Bird, B.W., 2007. Insolation forcing of Holocene  
811 climate change in Southern California: a sediment study from Lake Elsinore. *J.*  
812 *Paleolimnol.* 38, 395–417. doi:10.1007/s10933-006-9085-7
- 813 Kirby, M.E., Lund, S.P., Bird, B.W., 2006. Mid-Wisconsin sediment record from Baldwin Lake  
814 reveals hemispheric climate dynamics (Southern CA, USA). *Palaeogeogr.*  
815 *Palaeoclimatol. Palaeoecol.* 241, 267–283. doi:10.1016/j.palaeo.2006.03.043

- 816 Kirby, M.E., Zimmerman, S.R.H., Patterson, W.P., Rivera, J.J., 2012. A 9170-year record of  
 817 decadal-to-multi-centennial scale pluvial episodes from the coastal Southwest United  
 818 States: a role for atmospheric rivers? *Quat. Sci. Rev.* 46, 57–65.  
 819 doi:10.1016/j.quascirev.2012.05.008
- 820 Krantz, T., 1983. The Pebble Plains of Baldwin Lake. *Fremontia* 10, 9–13.
- 821 Kylander, M.E., Ampel, L., Wohlfarth, B., Veres, D., 2011. High-resolution X-ray fluorescence  
 822 core scanning analysis of Les Echets (France) sedimentary sequence: new insights from  
 823 chemical proxies. *J. Quat. Sci.* 26, 109–117. doi:10.1002/jqs.1438
- 824 Lachniet, M.S., Denniston, R.F., Asmerom, Y., Polyak, V.J., 2014. Orbital control of western  
 825 North America atmospheric circulation and climate over two glacial cycles. *Nat.*  
 826 *Commun.* 5. doi:10.1038/ncomms4805
- 827 Lawson, M.J., Roder, B.J., Stang, D.M., Rhodes, E.J., 2012. OSL and IRSL characteristics of  
 828 quartz and feldspar from southern California, USA. *Radiat. Meas.* 47, 830–836.  
 829 doi:10.1016/j.radmeas.2012.03.025
- 830 Leidy, R., 2006. Prehistoric and Historic Environmental Conditions in Bear Valley, San  
 831 Bernardino County, California. Sacramento, CA.
- 832 Li, J., Lowenstein, T.K., Brown, C.B., Ku, T.-L., Luo, S., 1996. A 100 ka record of water tables  
 833 and paleoclimates from salt cores, Death Valley, California. *Palaeogeogr. Palaeoclimatol.*  
 834 *Palaeoecol.* 123, 179–203. doi:10.1016/0031-0182(95)00123-9
- 835 Lin, J.C., Broecker, W.S., Hemming, S.R., Hajdas, I., Anderson, R.F., Smith, G.I., Kelley, M.,  
 836 Bonani, G., 1998. A Reassessment of U-Th and <sup>14</sup>C Ages for Late-Glacial High-  
 837 Frequency Hydrological Events at Searles Lake, California. *Quat. Res.* 49, 11–23.  
 838 doi:10.1006/qres.1997.1949
- 839 Lund, D.C., Mix, A.C., 1998. Millennial-scale deep water oscillations: Reflections of the North  
 840 Atlantic in the deep Pacific from 10 to 60 ka. *Paleoceanography* 13, 10–19.  
 841 doi:10.1029/97PA02984
- 842 Lyle, M., Heusser, L., Ravelo, C., Andreasen, D., Olivarez Lyle, A., Diffenbaugh, N., 2010.  
 843 Pleistocene water cycle and eastern boundary current processes along the California  
 844 continental margin. *Paleoceanography* 25. doi:10.1029/2009PA001836
- 845 MacDonald, G.M., Case, R.A., 2005. Variations in the Pacific Decadal Oscillation over the past  
 846 millennium. *Geophys. Res. Lett.* 32. doi:10.1029/2005GL022478
- 847 MacDonald, G.M., Moser, K.A., Bloom, A.M., Porinchu, D.F., Potito, A.P., Wolfe, B.B.,  
 848 Edwards, T.W.D., Petel, A., Orme, A.R., Orme, A.J., 2008. Evidence of temperature  
 849 depression and hydrological variations in the eastern Sierra Nevada during the Younger  
 850 Dryas stade. *Quat. Res.* 70, 131–140. doi:10.1016/j.yqres.2008.04.005
- 851 Mahan, S.A., Gray, H.J., Pigati, J.S., Wilson, J., Lifton, N.A., Paces, J.B., Blaauw, M., 2014. A  
 852 geochronologic framework for the Ziegler Reservoir fossil site, Snowmass Village,  
 853 Colorado. *Quat. Res.* 82, 490–503. doi:10.1016/j.yqres.2014.03.004
- 854 Maher, K., Ibarra, D.E., Oster, J.L., Miller, D.M., Redwine, J.L., Reheis, M.C., Harden, J.W.,  
 855 2014. Uranium isotopes in soils as a proxy for past infiltration and precipitation across  
 856 the western United States. *Am. J. Sci.* 314, 821–857. doi:10.2475/04.2014.01

- 857 McKay, N.P., Kaufman, D.S., Michelutti, N., 2008. Biogenic silica concentration as a high-  
 858 resolution, quantitative temperature proxy at Hallet Lake, south-central Alaska. *Geophys.*  
 859 *Res. Lett.* 35. doi:10.1029/2007GL032876
- 860 Melles, M., Brigham-Grette, J., Glushkova, O.Y., Minyuk, P.S., Nowaczyk, N.R., Hubberten,  
 861 H.-W., 2006. Sedimentary geochemistry of core PG1351 from Lake El'gygytgyn—a  
 862 sensitive record of climate variability in the East Siberian Arctic during the past three  
 863 glacial–interglacial cycles. *J. Paleolimnol.* 37, 89–104. doi:10.1007/s10933-006-9025-6
- 864 Mensing, S.A., Sharpe, S.E., Tunno, I., Sada, D.W., Thomas, J.M., Starratt, S., Smith, J., 2013.  
 865 The Late Holocene Dry Period: multiproxy evidence for an extended drought between  
 866 2800 and 1850 cal yr BP across the central Great Basin, USA. *Quat. Sci. Rev.* 78, 266–  
 867 282. doi:10.1016/j.quascirev.2013.08.010
- 868 Minnich, R.A., 1984. Snow Drifting and Timberline Dynamics on Mount San Gorgonio,  
 869 California, U.S.A. *Arct. Alp. Res.* 16, 395. doi:10.2307/1550901
- 870 Morton, D.M., Miller, F.K., 2006. Geologic map of the San Bernardino and Santa Ana 30' x 60'  
 871 quadrangles, California (Open-File No. 2006–1217). U. S. Geological Survey.
- 872 Moseley, G.E., Edwards, R.L., Wendt, K.A., Cheng, H., Dublyansky, Y., Lu, Y., Boch, R.,  
 873 Spotl, C., 2016. Reconciliation of the Devils Hole climate record with orbital forcing.  
 874 *Science* 351, 165–168. doi:10.1126/science.aad4132
- 875 Muhs, D.R., Simmons, K.R., Schumann, R.R., Groves, L.T., Mitrovica, J.X., Laurel, D., 2012.  
 876 Sea-level history during the Last Interglacial complex on San Nicolas Island, California:  
 877 implications for glacial isostatic adjustment processes, paleozoogeography and tectonics.  
 878 *Quat. Sci. Rev.* 37, 1–25. doi:10.1016/j.quascirev.2012.01.010
- 879 Nowaczyk, N.R., Melles, M., Minyuk, P., 2006. A revised age model for core PG1351 from  
 880 Lake El'gygytgyn, Chukotka, based on magnetic susceptibility variations tuned to  
 881 northern hemisphere insolation variations. *J. Paleolimnol.* 37, 65–76.  
 882 doi:10.1007/s10933-006-9023-8
- 883 Nussbaumer, S.U., Steinhilber, F., Trachsel, M., Breitenmoser, P., Beer, J., Blass, A., Grosjean,  
 884 M., Hafner, A., Holzhauser, H., Wanner, H., Zumbühl, H.J., 2011. Alpine climate during  
 885 the Holocene: a comparison between records of glaciers, lake sediments and solar  
 886 activity. *J. Quat. Sci.* 26, 703–713. doi:10.1002/jqs.1495
- 887 Oster, J.L., Ibarra, D.E., Winnick, M.J., Maher, K., 2015. Steering of westerly storms over  
 888 western North America at the Last Glacial Maximum. *Nat. Geosci.* 8, 201–205.  
 889 doi:10.1038/ngeo2365
- 890 Oster, J.L., Kelley, N.P., 2016. Tracking regional and global teleconnections recorded by  
 891 western North American speleothem records. *Quat. Sci. Rev.* 149, 18–33.  
 892 doi:10.1016/j.quascirev.2016.07.009
- 893 Oster, J.L., Montañez, I.P., Mertz-Kraus, R., Sharp, W.D., Stock, G.M., Spero, H.J., Tinsley, J.,  
 894 Zachos, J.C., 2014. Millennial-scale variations in western Sierra Nevada precipitation  
 895 during the last glacial cycle MIS 4/3 transition. *Quat. Res.* 82, 236–248.  
 896 doi:10.1016/j.yqres.2014.04.010

- 897 Overpeck, J., Garfin, G., Jardine, A., Busch, D.E., Cayan, D., Dettinger, M., Fleishman, E.,  
 898 Gershunov, A., MacDonald, G., Redmond, K.T., Travis, W.R., Udall, B., 2013. Summary  
 899 for Decision Makers, in: Garfin, G., Jardine, A., Merideth, R., Black, M., LeRoy, S.  
 900 (Eds.), *Assessment of Climate Change in the Southwest United States*. Island  
 901 Press/Center for Resource Economics, Washington, DC, pp. 1–20.
- 902 Overpeck, J., Udall, B., 2010. Dry Times Ahead. *Science* 328, 1642–1643.  
 903 doi:10.1126/science.1186591
- 904 Owen, L.A., Finkel, R.C., Minnich, R.A., Perez, A.E., 2003. Extreme southwestern margin of  
 905 late Quaternary glaciation in North America: Timing and controls. *Geology* 31, 729.  
 906 doi:10.1130/G19561.1
- 907 Pak, D.K., Lea, D.W., Kennett, J.P., 2012. Millennial scale changes in sea surface temperature  
 908 and ocean circulation in the northeast Pacific, 10-60 kyr BP: CA MARGIN  
 909 MILLENNIAL SCALE EVENTS. *Paleoceanography* 27, n/a-n/a.  
 910 doi:10.1029/2011PA002238
- 911 Paladino, L., 2008. A vegetation reconstruction of Big Bear Lake: local changes and inferred  
 912 regional climatology. UCLA, Los Angeles.
- 913 Phillips, F.M., Zreda, M.G., Benson, L.V., Plummer, M.A., Elmore, D., Sharma, P., 1996.  
 914 Chronology for Fluctuations in Late Pleistocene Sierra Nevada Glaciers and Lakes.  
 915 *Science* 274, 749–751. doi:10.1126/science.274.5288.749
- 916 Pigati, J.S., Bright, J.E., Shanahan, T.M., Mahan, S.A., 2009. Late Pleistocene paleohydrology  
 917 near the boundary of the Sonoran and Chihuahuan Deserts, southeastern Arizona, USA.  
 918 *Quat. Sci. Rev.* 28, 286–300. doi:10.1016/j.quascirev.2008.09.022
- 919 Pigati, J.S., Miller, D.M., Bright, J.E., Mahan, S.A., Nekola, J.C., Paces, J.B., 2011. Chronology,  
 920 sedimentology, and microfauna of groundwater discharge deposits in the central Mojave  
 921 Desert, Valley Wells, California. *Geol. Soc. Am. Bull.* 123, 2224–2239.  
 922 doi:10.1130/B30357.1
- 923 Pospelova, V., Price, A.M., Pedersen, T.F., 2015. Palynological evidence for late Quaternary  
 924 climate and marine primary productivity changes along the California margin: CLIMATE  
 925 AND PRIMARY PRODUCTIVITY ON CM. *Paleoceanography* 30, 877–894.  
 926 doi:10.1002/2014PA002728
- 927 Price, A.M., Mertens, K.N., Pospelova, V., Pedersen, T.F., Ganeshram, R.S., 2013. Late  
 928 Quaternary climatic and oceanographic changes in the Northeast Pacific as recorded by  
 929 dinoflagellate cysts from Guaymas Basin, Gulf of California (Mexico):  
 930 DINOFLAGELLATE CYSTS FROM GUAYMAS BASIN. *Paleoceanography* 28, 200–  
 931 212. doi:10.1002/palo.20019
- 932 Prokopenko, A.A., Hinnov, L.A., Williams, D.F., Kuzmin, M.I., 2006. Orbital forcing of  
 933 continental climate during the Pleistocene: a complete astronomically tuned climatic  
 934 record from Lake Baikal, SE Siberia. *Quat. Sci. Rev.* 25, 3431–3457.  
 935 doi:10.1016/j.quascirev.2006.10.002
- 936 Rack, F.R., Heise, E.A., Stein, R., 1995. MAGNETIC SUSCEPTIBILITY AND PHYSICAL  
 937 PROPERTIES OF SEDIMENT CORES FROM SITE 893, SANTA BARBARA BASIN:  
 938 RECORDS OF SEDIMENT DIAGENESIS OR OF PALEOCLIMATIC AND

- 939 PALEOCEANOGRAPHIC CHANGE?., in: In Proceedings of the Ocean Drilling  
 940 Program, Scientific Results.
- 941 Rasmussen, S.O., Bigler, M., Blockley, S.P., Blunier, T., Buchardt, S.L., Clausen, H.B.,  
 942 Cvijanovic, I., Dahl-Jensen, D., Johnsen, S.J., Fischer, H., Gkinis, V., Guillevic, M.,  
 943 Hoek, W.Z., Lowe, J.J., Pedro, J.B., Popp, T., Seierstad, I.K., Steffensen, J.P., Svensson,  
 944 A.M., Vallelonga, P., Vinther, B.M., Walker, M.J.C., Wheatley, J.J., Winstrup, M., 2014.  
 945 A stratigraphic framework for abrupt climatic changes during the Last Glacial period  
 946 based on three synchronized Greenland ice-core records: refining and extending the  
 947 INTIMATE event stratigraphy. *Quat. Sci. Rev.* 106, 14–28.  
 948 doi:10.1016/j.quascirev.2014.09.007
- 949 Reheis, M.C., Miller, D.M., McGeehin, J.P., Redwine, J.R., Oviatt, C.G., Bright, J., 2015.  
 950 Directly dated MIS 3 lake-level record from Lake Manix, Mojave Desert, California,  
 951 USA. *Quat. Res.* 83, 187–203. doi:10.1016/j.yqres.2014.11.003
- 952 Reimer, P., 2013. IntCal13 and Marine13 Radiocarbon Age Calibration Curves 0–50,000 Years  
 953 cal BP. *Radiocarbon* 55, 1869–1887. doi:10.2458/azu\_rc.55.16947
- 954 Retelle, M., Child, J., 1996. Suspended sediment transport and deposition in a high arctic  
 955 meromictic lake. *J. Paleolimnol.* 16. doi:10.1007/BF00176933
- 956 Rhodes, E.J., 2015. Dating sediments using potassium feldspar single-grain IRSL: Initial  
 957 methodological considerations. *Quat. Int.* 362, 14–22. doi:10.1016/j.quaint.2014.12.012
- 958 Rood, D.H., Burbank, D.W., Finkel, R.C., 2011. Chronology of glaciations in the Sierra Nevada,  
 959 California, from <sup>10</sup>Be surface exposure dating. *Quat. Sci. Rev.* 30, 646–661.  
 960 doi:10.1016/j.quascirev.2010.12.001
- 961 Roy, P.D., Quiroz-Jiménez, J.D., Pérez-Cruz, L.L., Lozano-García, S., Metcalfe, S.E., Lozano-  
 962 Santacruz, R., López-Balbiaux, N., Sánchez-Zavala, J.L., Romero, F.M., 2013. Late  
 963 Quaternary paleohydrological conditions in the drylands of northern Mexico: a summer  
 964 precipitation proxy record of the last 80 cal ka BP. *Quat. Sci. Rev.* 78, 342–354.  
 965 doi:10.1016/j.quascirev.2012.11.020
- 966 Schnurrenberger, D., Russell, J., Kelts, K., 2003. Classification of lacustrine sediments based on  
 967 sedimentary components. *J. Paleolimnol.* 29, 141–154. doi:10.1023/A:1023270324800
- 968 Seki, O., Ishiwatari, R., Matsumoto, K., 2002. Millennial climate oscillations in NE Pacific  
 969 surface waters over the last 82 kyr: New evidence from alkenones: ALKENONE SEA  
 970 SURFACE TEMPERATURE IN CALIFORNIA MARGIN. *Geophys. Res. Lett.* 29, 59-  
 971 1-59-4. doi:10.1029/2002GL015200
- 972 Silveira, E.I., 2014. Reconstructing hydrologic change over the past 96,000 years using  
 973 sediments from Baldwin Lake, San Bernardino County, California (B.A. Thesis). CSU-  
 974 Fullerton, Fullerton, CA.
- 975 Springer, K.B., Manker, C.R., Pigati, J.S., 2015. Dynamic response of desert wetlands to abrupt  
 976 climate change. *Proc. Natl. Acad. Sci.* 112, 14522–14526. doi:10.1073/pnas.1513352112
- 977 Stout, M.L., 1976. Geologic Guide to the San Bernardino Mountains, Southern California:  
 978 Annual Spring Field Trip.

- 979 Street, J.H., Anderson, R.S., Paytan, A., 2012. An organic geochemical record of Sierra Nevada  
 980 climate since the LGM from Swamp Lake, Yosemite. *Quat. Sci. Rev.* 40, 89–106.  
 981 doi:10.1016/j.quascirev.2012.02.017
- 982 Tubbs, A.M., 1972. Summer Thunderstorms Over Southern California. *Mon. Weather Rev.* 100,  
 983 799–807. doi:10.1175/1520-0493(1972)100<0799:STOSC>2.3.CO;2
- 984 Tzedakis, P.C., Andrieu, V., de Beaulieu, J.-L., Birks, H.J.B., Crowhurst, S., Follieri, M.,  
 985 Hooghiemstra, H., Magri, D., Reille, M., Sadori, L., Shackleton, N.J., Wijmstra, T.A.,  
 986 2001. Establishing a terrestrial chronological framework as a basis for biostratigraphical  
 987 comparisons. *Quat. Sci. Rev.* 20, 1583–1592. doi:10.1016/S0277-3791(01)00025-7
- 988 U.S. Climate Data [WWW Document], 2016. . US Clim. Data Big Bear Lake - Calif. URL  
 989 <http://www.usclimatedata.com/climate/big-bear-lake/california/united-states/usca0094>  
 990 (accessed 8.8.16).
- 991 Vogel, H., Meyer-Jacob, C., Melles, M., Brigham-Grette, J., Andreev, A.A., Wennrich, V.,  
 992 Tarasov, P.E., Rosén, P., 2013. Detailed insight into Arctic climatic variability during  
 993 MIS 11c at Lake El'gygytgyn, NE Russia. *Clim. Past* 9, 1467–1479. doi:10.5194/cp-9-  
 994 1467-2013
- 995 Wagner, J.D.M., Cole, J.E., Beck, J.W., Patchett, P.J., Henderson, G.M., Barnett, H.R., 2010.  
 996 Moisture variability in the southwestern United States linked to abrupt glacial climate  
 997 change. *Nat. Geosci.* 3, 110–113. doi:10.1038/ngeo707
- 998 Wise, E.K., 2010. Spatiotemporal variability of the precipitation dipole transition zone in the  
 999 western United States: PRECIPITATION DIPOLE TRANSITION ZONE. *Geophys. Res.*  
 1000 *Lett.* 37, n/a-n/a. doi:10.1029/2009GL042193
- 1001 Wohlfarth, B., Veres, D., Ampel, L., Lacourse, T., Blaauw, M., Preusser, F., Andrieu-Ponel, V.,  
 1002 Kéravis, D., Lallier-Vergès, E., Björck, S., Davies, S.M., de Beaulieu, J.-L., Risberg, J.,  
 1003 Hormes, A., Kasper, H.U., Possnert, G., Reille, M., Thouveny, N., Zander, A., 2008.  
 1004 Rapid ecosystem response to abrupt climate changes during the last glacial period in  
 1005 western Europe, 40–16 ka. *Geology* 36, 407. doi:10.1130/G24600A.1
- 1006 Woodhouse, C.A., Meko, D.M., MacDonald, G.M., Stahle, D.W., Cook, E.R., 2010. A 1,200-  
 1007 year perspective of 21st century drought in southwestern North America. *Proc. Natl.*  
 1008 *Acad. Sci.* 107, 21283–21288. doi:10.1073/pnas.0911197107
- 1009 Woolfenden, W.B., 2003. A 180,000-year pollen record from Owens Lake, CA: terrestrial  
 1010 vegetation change on orbital scales. *Quat. Res.* 59, 430–444. doi:10.1016/S0033-  
 1011 5894(03)00033-4
- 1012 Zimmerman, S.H., Myrbo, A., 2015. Lacustrine Environments (14 C)., in: *Encyclopedia of*  
 1013 *Scientific Dating Methods*. pp. 365–371.
- 1014 Zimmerman, S.R.H., Pearl, C., Hemming, S.R., Tamulonis, K., Hemming, N.G., Searle, S.Y.,  
 1015 2011. Freshwater control of ice-rafted debris in the last glacial period at Mono Lake,  
 1016 California, USA. *Quat. Res.* 76, 264–271. doi:10.1016/j.yqres.2011.06.003
- 1017

Table 1. AMS radiocarbon dates, infrared-stimulated luminescence dates, and tie points used for BDL12's age model. Mean age from Bacon 2.2 (based upon IntCal13; Reimer et al., 2013) is used for the calendar-years age model; see text and Figure 2 for details.

<b>Accelerated Mass Spectrometry Radiocarbon Dates</b>				
W. M. Keck Carbon Cycle AMS Radiocarbon Lab, UC-Irvine				
<b>Sample No.</b>	<b>Depth (cm)</b>	<b>Material</b>	<b>Raw <sup>14</sup>C Age</b>	<b>Approximate Calendar Age</b>
UCI-121791	152	charcoal	10,010 ± 320	~11,868
UCI-124533	262	charcoal	21,150 ± 810	~24,307
UCI-124534	389	charcoal	25,170 ± 280	~29,339
UCI-121792	440	pine cone piece	25,990 ± 140	~30,400
UCI-124535	529	charcoal	27,240 ± 180	~31,474
UCI-124536	745	charcoal	35,710 ± 790	~40,417
UCI-121793	815	twig	41,010 ± 700	~43,997
<b>Post-IR Infrared Stimulated Luminescence dates</b>				
Earth and Planetary Sciences Dept., UCLA				
<b>Sample No.</b>	<b>Depth (cm)</b>	<b>Material</b>	<b>50°C IRSL Signal (cal yr BP)</b>	<b>225°C IRSL Signal (cal yr BP)</b>
J0395	2075	massive silt	88,500 ± 6,200	87,800 ± 6,100
J0396	2173	clayey silt	55,800 ± 5,400	44,900 ± 3,900
J0397	2570	sand	117,000 ± 8,000	109,000 ± 8,000
J0398	2700	sand	136,000 ± 10,000	124,000 ± 8,000
<b>Tie-Points for orbital tuning</b>				
	<b>Depth (cm)</b>			<b>Age (cal yr BP)</b>
	1573			71,000
	1746			83,000
	2060			94,000
	2197			105,000
	2433			116,000

**Table 2.** Multi-proxy summary from Baldwin Lake core BDL12, by Marine Isotope Stage (MIS). MS = magnetic susceptibility, reported in SI units ( $10^5$  of measured values).  $\text{CaCO}_3$  = carbonate content from loss-on-ignition analysis. Trace element data (Ca, Fe, Ti, and Mn:Ti) reported as average ppm for each MIS, unless otherwise noted. “Insolation” refers to summer insolation at  $30^\circ\text{N}$  (Laskar, 2004), except for MIS 3, where both summer and winter are noted. For MIS 5, substages with letters (e.g. MIS 5b) refer to the span of the entire substage and its conditions, and are ordered alphabetically youngest-to-oldest.

Stage/Substages Cal Yr BP	Key Changes in Insolation and Proxy Data	Key Paleoenvironmental Conditions/Events
MIS 5e (125 to 120)	<ul style="list-style-type: none"> <li>relatively rapid insolation shift from <math>528 \text{ W/m}^2</math> at 127 ka, to <math>474 \text{ W/m}^2</math> at 120 ka</li> <li>sand facies throughout (grain size mode <math>&gt;400 \mu\text{m}</math>); minimal clay (<math>&lt;1\%</math>)</li> <li>high dry density (<math>&gt;1.2 \text{ g/cm}^3</math>), MS <math>&lt;7</math> SI throughout; average value 3.2 SI</li> <li>Ti (<math>\sim 2400</math> ppm) and Fe (<math>\sim 8500</math> ppm) low until rapid increase to 3500 ppm (Ti) and <math>&gt;20,000</math> ppm (Fe) at 121 ka</li> <li>low organic content (<math>&lt;1\%</math>), <math>\text{CaCO}_3</math> (<math>&lt;3\%</math>) and Ca (<math>\sim 6800</math> ppm) throughout; no BSi analysis</li> </ul>	<ul style="list-style-type: none"> <li>High-energy deposition</li> </ul>
MIS 5d – 5c (120 to 95)	<ul style="list-style-type: none"> <li>insolation low <math>448 \text{ W/m}^2</math> at 116 ka, rose to <math>533 \text{ W/m}^2</math> by 105 ka, declined to <math>460 \text{ W/m}^2</math> by 95 ka</li> <li>fine-grained, inorganic clayey silt throughout, with fine sand (grain size mode = <math>58 \mu\text{m}</math>) at 106 ka</li> <li>MS rose from <math>\sim 7</math> SI to <math>\sim 16</math> SI from 121 - 118 ka, gradually declined to <math>&lt;5</math> SI by 112 ka, generally stayed below <math>&lt;6</math> SI until 95 ka, except for short excursion at 101 ka (51 SI)</li> <li>high Ti (<math>\sim 3500</math> ppm) and Fe (<math>\sim 35,000</math> ppm) until 112 ka, lows of <math>\sim 600</math> ppm (Ti) and <math>\sim 8000</math> ppm (Fe) at 107 and 102 ka, moderate-to-high Ti (<math>\sim 2500</math> ppm) and Fe (<math>\sim 25,000</math> ppm) began 98 ka</li> <li>low-to-moderate Ca (<math>\sim 20,000</math> ppm) and <math>\text{CaCO}_3</math> (5000-10,000 ppm) until peak at 112 ka (Ca <math>\sim 109,000</math> ppm, <math>\text{CaCO}_3</math> <math>\sim 20\%</math>), then declined over next 8 kyr until 95 ka</li> <li>low organics (<math>&lt;5\%</math>) until 113 ka, peaks <math>\sim 33</math>-<math>39\%</math> at 106 ka and 103 ka, declined to <math>&lt;5\%</math> by 95 ka</li> <li>BSi generally followed organics, with 1-3 mg/g background, peak of 11.3 mg/g at 103 ka</li> </ul>	<ul style="list-style-type: none"> <li>Basin closure near onset of MIS 5d</li> <li>Cool, deep, unproductive lake conditions ascribed to MIS 5d insolation minimum</li> <li>High-erosion event 106 ka</li> <li>Transition to more shallow, productive lake late MIS 5d; peak productivity during MIS 5c (103 ka)</li> </ul>
MIS 5b – 5a (95 to 71)	<ul style="list-style-type: none"> <li>insolation rose from <math>460 \text{ W/m}^2</math> at 95 ka to <math>524 \text{ W/m}^2</math> by 83 ka; declined to <math>465 \text{ W/m}^2</math> by 72-71 ka</li> <li>silt deposition throughout, with calcareous layers including mollusks that end abruptly 81 ka</li> <li>MS low (<math>&lt;2</math> SI) between 86 – 76 ka; rose to 5 – 7 SI by end of MIS 5</li> <li>moderate Ti (<math>\sim 1200</math> ppm) and Fe (17,000 ppm) at 95 ka, declined to <math>&lt;100</math> ppm and <math>\sim 6000</math> ppm by 83 ka, gradually increased to 1700 ppm and 18,000 ppm by 71 ka.</li> <li>moderate Ca (25,000 – 60,000 ppm) until 89 ka, then maxima 180,000 ppm at 86 ka, and 160,000 ppm at 83 ka. <math>\text{CaCO}_3</math> ranged 5-15%, with peaks 22% at 86 ka, and 30% at 83 ka. Mn:Ti 0.84 at 83 ka and 0.74 c. 86 ka.</li> <li>varied organic content: minima are <math>&lt;5\%</math> from 95 – 93 ka and 73 – 72.6 ka, maxima of <math>\sim 33\%</math> at 88.2 ka and 81.6 ka. Maximum for BDL12 is 44% at the MIS 5a/MIS 4 transition (71 ka)</li> <li>BSi varied with organics, with peak value 17.4 mg/g at 82.6 ka</li> </ul>	<ul style="list-style-type: none"> <li>High-amplitude change in lake productivity</li> <li>Lowstand conditions evident at 87 ka and 82 ka, with abrupt transition out of the latter, likely due to rapid shift in available moisture</li> </ul>



MIS 4 (71 to 57)	<ul style="list-style-type: none"> <li>• low insolation 465 W/m<sup>2</sup> at 71 ka increased to 510 W/m<sup>2</sup> by 60 ka</li> <li>• clayey silt (density ~0.70 g/cm<sup>3</sup>) deposition that transitioned to organic silt (density &lt;0.54 g/cm<sup>3</sup>)</li> <li>• moderate-to-high organics (average = 16.5%); BSi at late MIS 4 (55-51 ka) was 9.8 – 11.5 mg/g</li> <li>• moderate-to-low MS, Ti and Fe throughout (MS ~5.0 SI, Ti ~1500 ppm, Fe ~20,000 ppm)</li> <li>• shallow-water indicators were moderate at onset of MIS 4: Ca (22,000 ppm), CaCO<sub>3</sub> (&lt;11%), but decline by 69 ka and remain low (Ca ~ 4900 ppm, CaCO<sub>3</sub> &lt;5%, Mn:Ti ~0.11),</li> </ul>	<ul style="list-style-type: none"> <li>• Basin shift occurred 69 ka towards deeper lake and sustained productivity that persisted after MIS 4</li> </ul>
MIS 3 (57 to 29)	<ul style="list-style-type: none"> <li>• summer insolation ranged between 481 – 506 W/m<sup>2</sup>; winter insolation 213 – 227 W/m<sup>2</sup> and maintained 220 W/m<sup>2</sup> from 49 to 37 ka</li> <li>• fine-grained organic silt (mode 12 – 39 μm), dry density &lt;1.00 g/cm<sup>3</sup> (average = 0.48 g/cm<sup>3</sup>)</li> <li>• low MS (average = 3.9 SI); Ti decreased from ~1700 to 900 ppm by 37 ka, then increased to ~1400 ppm by 29 ka. Broad decrease and increase in Fe (ranged ~11,000 – 21,000 ppm) with shorter, rapid increases throughout (~ 51,000 ppm)</li> <li>• suppressed Ca (~2500 ppm) and CaCO<sub>3</sub> (&lt;10%, average of ~4.3%) throughout MIS 3</li> <li>• moderate organic content (average = 18.8%), with millennial-scale fluctuations ranging 10—28%</li> <li>• BSi relatively high throughout MIS 3, ranging 7.7 – 13.4 mg/g</li> </ul>	<ul style="list-style-type: none"> <li>• lowest-amplitude variation in both summer and winter insolation for nearly 30 kyr; reduced seasonality</li> <li>• Consistently productive lake that remained stratified and deep</li> <li>• Organic content does not shift in tandem with summer insolation, and millennial-scale fluctuations suggest North Atlantic forcing (Figure 5)</li> </ul>
MIS 2 (29 to 14)	<ul style="list-style-type: none"> <li>• insolation low of 471 W/m<sup>2</sup> at 23 ka, reached 509 W/m<sup>2</sup> by 14 ka</li> <li>• predominantly silt deposition, with a coarser layer (28% sand) 28 ka; deposition rate declined by more than half (~0.05 cm/yr during MIS 3 to ~0.02 cm/yr for MIS 2m)</li> <li>• MS maximum at LGM start, with peak at 26 ka (~100 SI) above background values of 0 – 11 SI</li> <li>• high Ti (2300 – 3600 ppm) and Fe (average 26,000 ppm, with 56,000 ppm peak) began 26.3 ka, maintained until MIS 1</li> <li>• low Ca (6000 ppm), CaCO<sub>3</sub> (generally &lt;5%) and Mn:Ti (0.12) throughout</li> <li>• final organic content increase to 23% at 27.7 ka, then decline to &lt;5% by 21 ka and thereafter</li> <li>• BSi decreased overall from 7.9 to 5.4 mg/g, though with peaks and lags separate from organics. Pediastrum are abundant 24 ka, and trace element phosphorus began increase 27 ka from ~7000 ppm, reaching ~14,000 ppm by 14.5 ka</li> </ul>	<ul style="list-style-type: none"> <li>• Low insolation, cold conditions, and deep water</li> <li>• last phase of moderate productivity at 27.7 ka not paced with insolation</li> <li>• BSi suggests moderate-to-low lake productivity during MIS 2, perhaps due to high K influx and abundant Pediastrum 24 ka</li> </ul>
MIS 1 (<14)	<ul style="list-style-type: none"> <li>• insolation continued its increase to 515 W/m<sup>2</sup> by 11 ka, declined to 488 W/m<sup>2</sup> by 5 ka</li> <li>• desiccated, inorganic clayey silt (mode grain size &lt;29μm); dry density is high (0.67 – 1.74 g/cm<sup>3</sup>)</li> <li>• erratic MS, varying between -2.6 - 8 SI; high Ca (~84,000 ppm), low Ti (~1300 ppm), generally low Fe (18,000 ppm) with excursion ~73,000 ppm at 11.8 ka, high Mn:Ti (0.58)</li> <li>• relatively high carbonate content; abrupt rise at 12.7 ka to ~15%; MIS 1 average 14.6%</li> <li>• low organic content (&lt;10%, average 4.7%) and two moderate BSi horizons (4.5 – 7.8 mg/g)</li> </ul>	<ul style="list-style-type: none"> <li>• Transition to intermittent lake</li> <li>• Desiccation, low sedimentation, and uncertain age prevent study of lake conditions after c. 12 ka</li> </ul>

Figure1

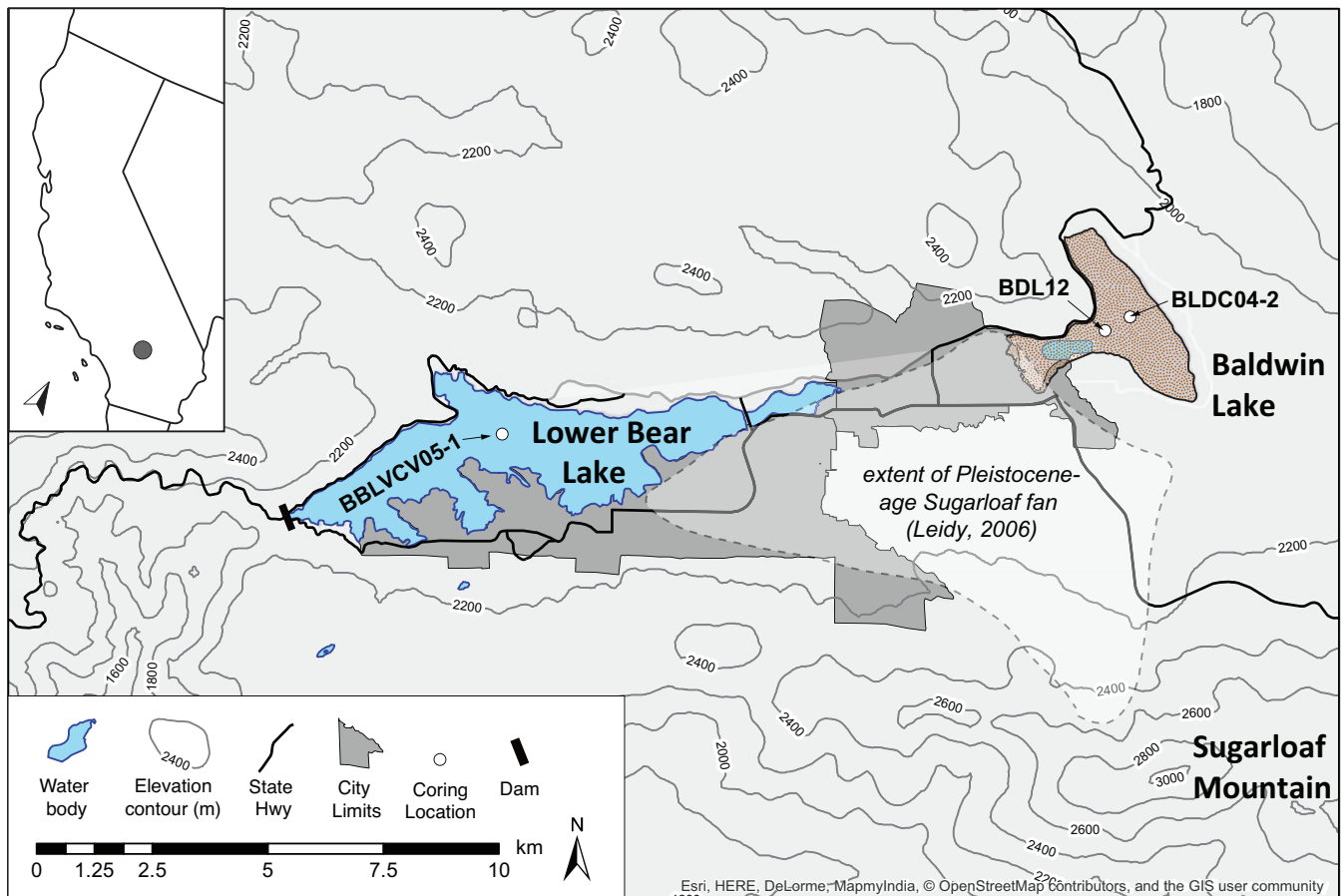


Figure2

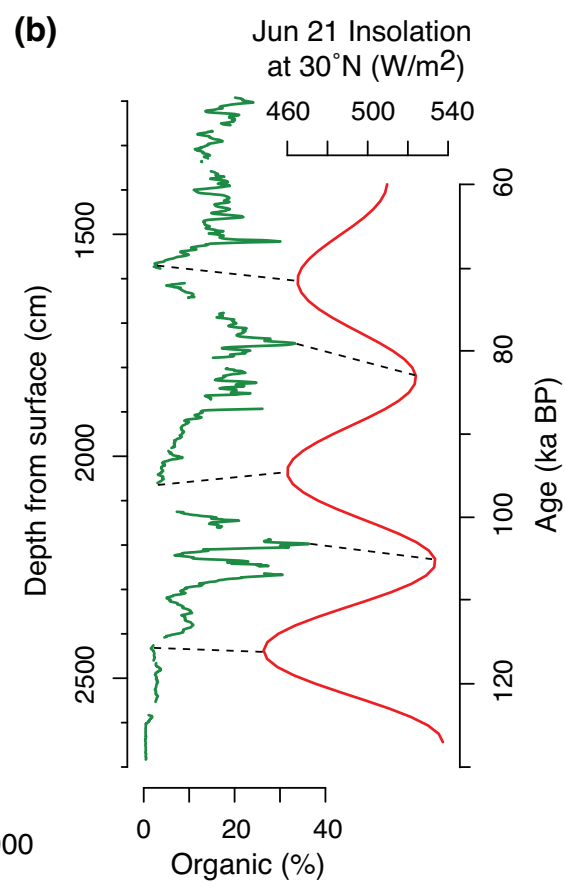
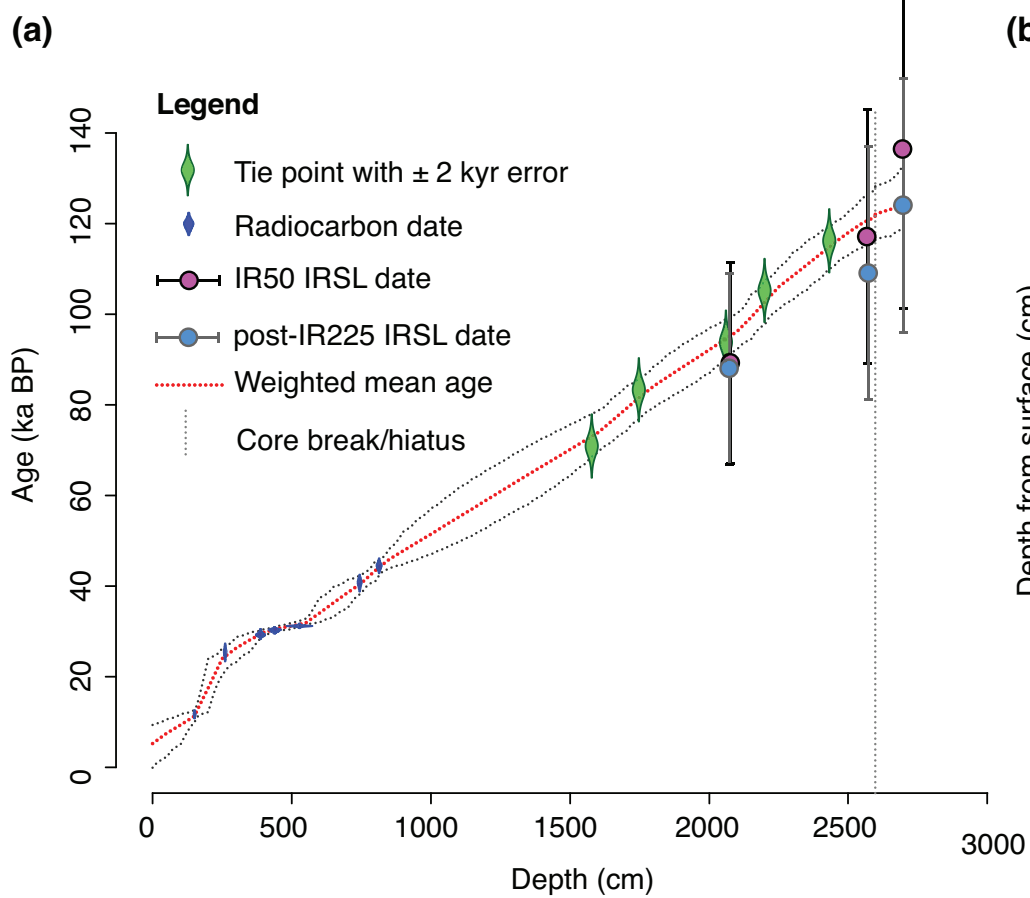


Figure 3

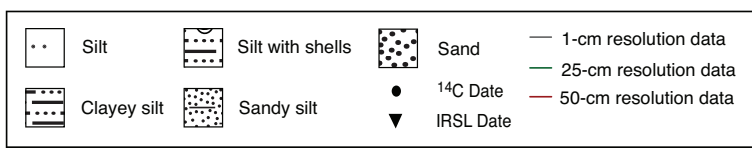
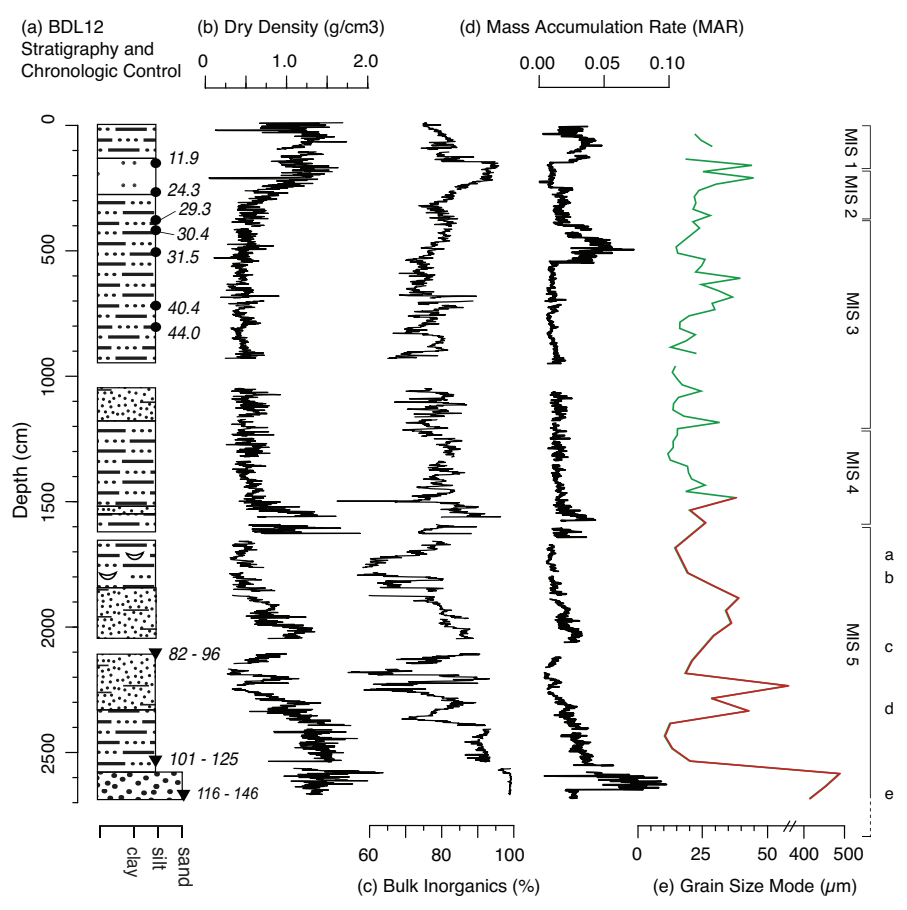
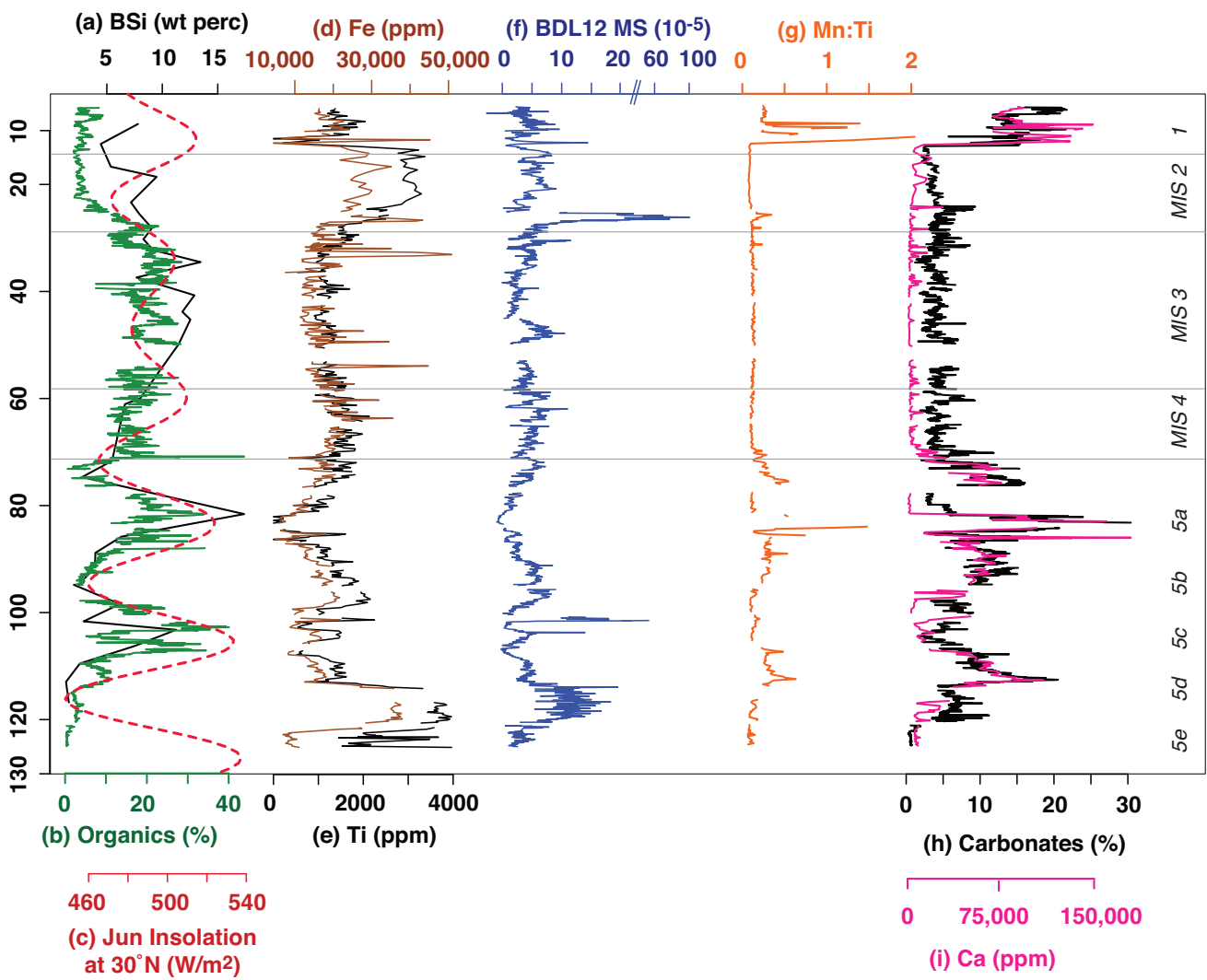


Figure4



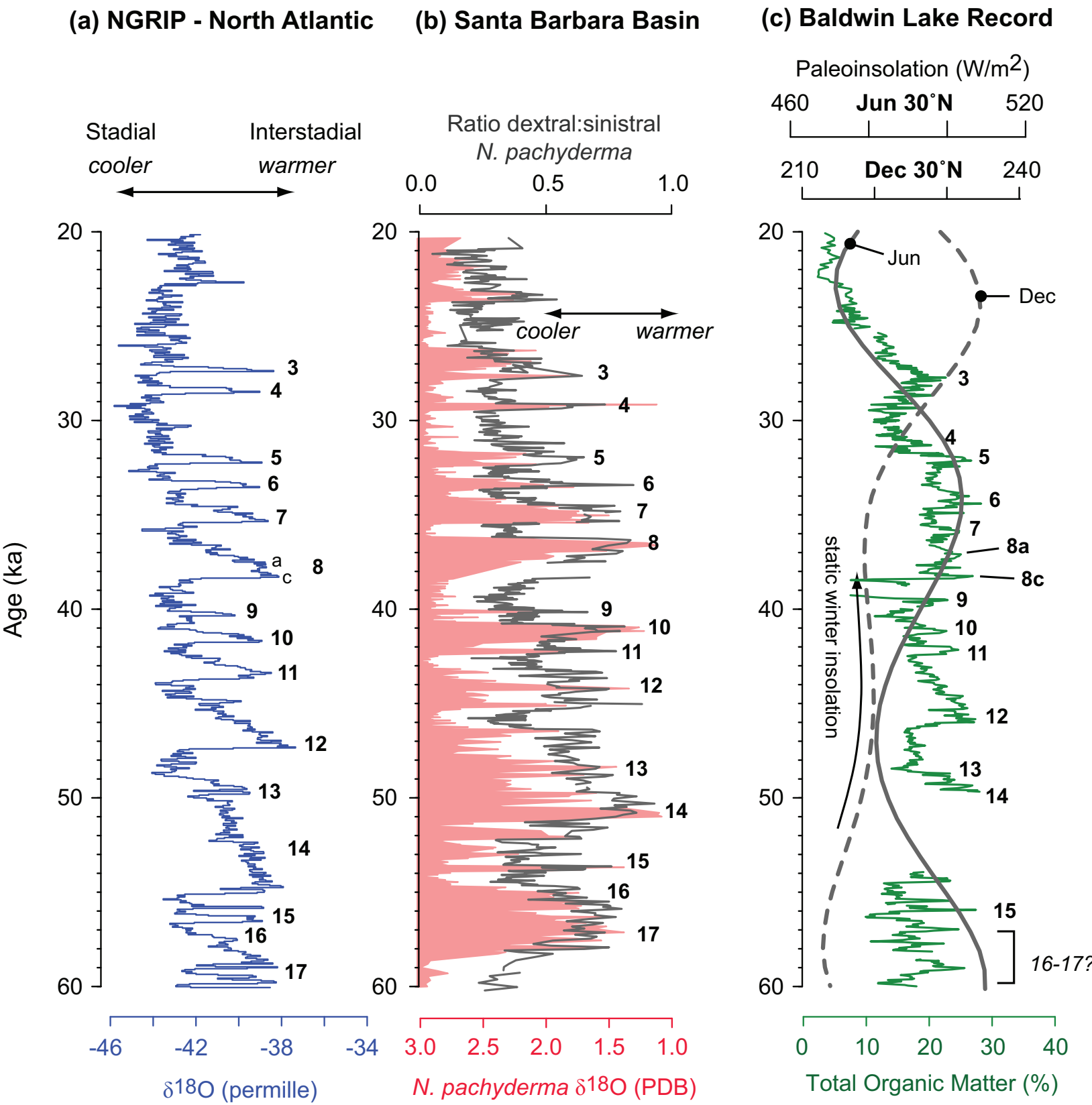


Figure 6

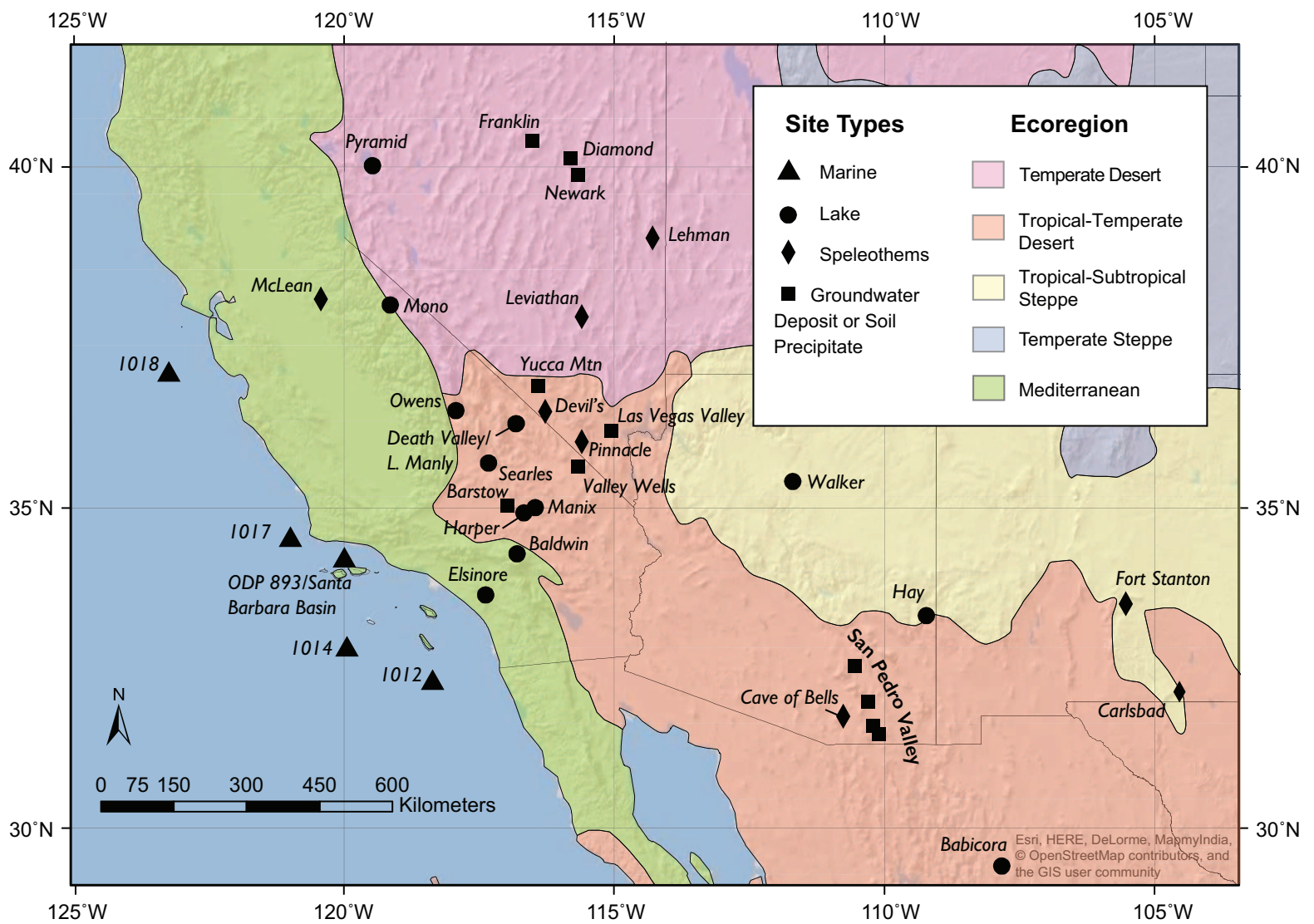


Figure7

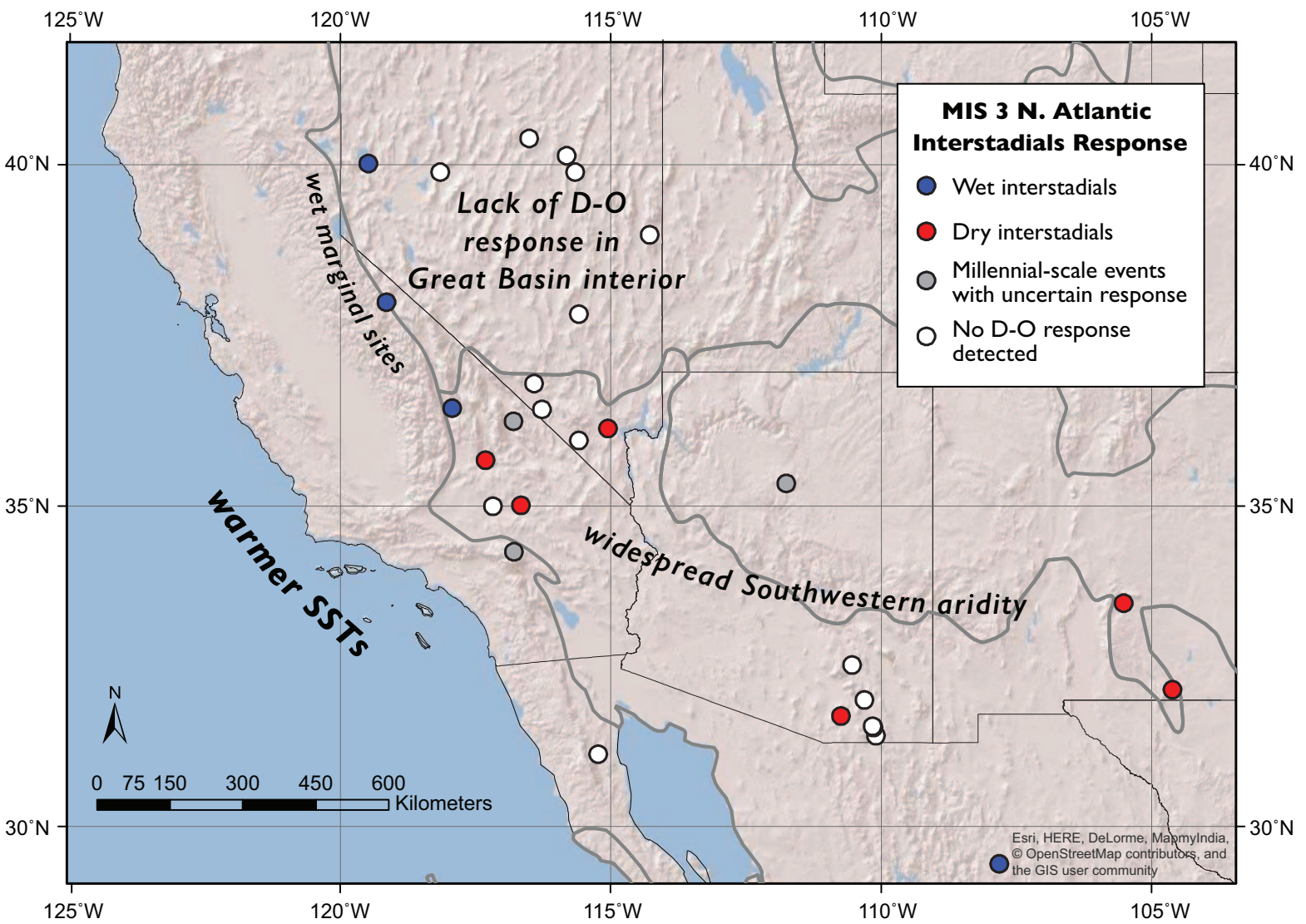




Figure 1. Map of Big Bear Valley, San Bernardino Mountains, California. Cores taken in include Lower Bear Lake (BBLVCV05-1; Kirby et al., 2012), Baldwin Lake (BDLC04-2; Kirby et al., 2006; Blazevic et al., 2009) and a second core from Baldwin Lake (BDL12; this study). Contour interval = 200 m

Figure 2. a) Bacon 2.2 age-depth model from radiocarbon dates, luminescence dates, and tie-points (Table 1). b) Tie-points established between insolation peaks and troughs from summer values at 30°N (Laskar, 2004), and corresponding maxima and minima in a 5-point moving average of high-resolution organic content data throughout BDL12.

Figure 3. Stratigraphy, age horizons, and sedimentological data for BDL12, with approximate boundaries of Marine Isotope Stages after Lisiecki and Raymo (2005). The age range for three pairs of post-IR IRSL dates are shown. Substage lettering (MIS 5e – 5a) is not bracketed at specific time points, due to this age uncertainty.

Figure 4. Physical and geochemical data, plotted by age and with Marine Isotope Stage boundaries noted. (a) Biogenic silica. (b) Bulk organic content, determined with loss-on-ignition. (c) Summer insolation at 30°N. (d) Trace element iron (Fe). (e) Trace element titanium (Ti). (f) BDL12 magnetic susceptibility (SI). (g) Manganese to titanium ratio (Mn:Ti). (h) Bulk carbonate content (CaCO<sub>3</sub>), determined with loss-on-ignition. (i) Trace element calcium (Ca).

Figure 5. (a) NGRIP  $\delta^{18}\text{O}$  shifts from 60 – 20 ka, with Greenland Interstadial (GI) numbers (i.e. Dansgaard-Oeschger events, Rasmussen et al., 2014). While many GIs have substages, only GI-8 has the substages shown for simplicity's sake. (b) Santa Barbara Basin core ODP-893, with interstadials labeled after Hendy and Kennett (2000) and latest age model (Hendy et al., 2007). (c) Baldwin Lake core BDL12 bulk organic content from 60 – 20 ka, with summer and winter insolation (Laskar, 2004), and proposed D-O interstadial numbering.

Figure 6. Paleoclimatic sites discussed in this review, with North American ecoregions shown (Bailey, 2009). See text for references.

Figure 7. Response of regional sites to Dansgaard-Oeschger (D-O) interstadials during MIS 3 (57 – 29 ka).

Highlights:

- A new multi-proxy record from Baldwin Lake, San Bernardino Mountains, California dates from 125-10 ka.
- Baldwin Lake's changes in primary productivity, determined with correlated loss-on-ignition and biogenic silica, were likely influenced over long timescales by subtropical summer insolation.
- Shorter, millennial-scale oscillations in primary productivity at Baldwin Lake coincide with Dansgaard-Oeschger events in the North Atlantic, and those detected at other California records.
- We thus hypothesize that alpine Southern California climate is sensitive to orbitally-induced insolation shifts, and rapid climate change in the North Atlantic.
- A review of paleoclimate sites throughout Southern California, the Great Basin, and the Southwest show that widespread hydrologic state change occurred at the MIS 4/3 transition (60 – 57 ka), and Dansgaard-Oeschger events during MIS 3 coincide with warmer SSTs, and enhanced aridity in Southern California and Southwestern deserts.



## **Response to Reviewers for QSR submission #JQSR-D-16-00445R1**

(Glover et al., "Evidence for orbital and North Atlantic climate forcing in alpine Southern California between 125 - 10 ka from multi-proxy analyses of Baldwin Lake")

*Response to individual comments re. numbered lines of manuscript are in italics. Please note that the line numbering of the resubmitted manuscript is different in most places.*

### Reviewer #1: Major comments

The revised manuscript by Glover et al is improved from the previous version, and has significantly clearer conclusion. The science is pretty solid. I don't see any scientific issues that are barriers to the work being eventually published in QSR.

But the writing still needs substantial improvement, as detailed extensively below. I had hoped the senior authors would have spent some more time (so the volunteer reviewers didn't need to) helping to improve the writing, but there are so many typos and unclear sentences that it seems this hasn't happened extensively.

In general, a useful pro-tip for writing is to provide context and rationale before a conclusion. Here's an example of how line 150-1 could be improved to make the writing clearer: "Because a significant correlation between BSi - which is primarily produced in lake waters - and organic content can best be explained by in situ lake productivity, the observed correlation ( $r = 0.80$ ) between them at Baldwin Lake supports our interpretation that organic content does not reflect an influx of terrestrial organic material into the lake". Remember that your reasoning is not always apparent to the reader, who may not be a specialist in paleolimnology. Examples abound throughout the manuscript that would benefit from similar improvements. I've tried to provide a few prominent examples.

*Thank you for the careful read-through for suggested examples. We have looked thoroughly through the manuscript for typos and unclear sentences. We also have made use of the suggested structure (context->rationale->conclusion) as noted below.*

### Minor comments

L44: change to "Pacific southwest"? Sounds better than "coastal" and has a better-known counterpart in Pacific Northwest.

*"U.S. Coastal Southwest" has been a problematic phrase while writing this paper. Southern California seems the best, most clear way to name the area discussed in this section. This is referenced in the previous sentence. This sentence noted here has been changed to just say "towards the coast" to differentiate it from interior desert regions.*

L78 needs some context to begin, like "Following initial short-core extractions in 200x,..."

*I interpreted this to mean: provide context of prior work on the site. I added a lead-in sentence referencing Matt Kirby's coring and work at Baldwin Lake from 2004-2006.*

116: needs some clarification. Describe why would BSi not reflect terrestrial input, provide context for the reader. I would rephrase this sentence along the lines of "Because BSi is only produced within lake waters, a significant correlation to organic content would indicate that lake primary productivity, not influx of terrestrial organic material from the watershed, is the dominant control of organic production".

*This section has been rephrased, utilizing some of the suggested language. Some nuance was necessary, however, and emerged from discussion between the authors about BSi as a proxy. High primary productivity can derive from both enhanced light intensity and terrestrial runoff (which will lead to enhanced nutrient loading, and terrestrial sources of amorphous silica e.g. phytoliths, though these tend to be minimal).*

*I aimed to keep interpretative statements about the proxy limited in the "Methods" section where I could. The exception to this is the ensuing "Chronologic Control" section (3.4), where I did feel this was important to discuss lake processes, as this understanding is important for the assumptions made. I changed the name of 3.4 to "Chronologic Control – assumptions and approach" to signal that this is a longer-than-usual discussion for "Methods." Section 4.3 later in the paper was also written with the original intend of interpreting and defending how proxies are responding in this particular basin, given the evidence and literature.*

140-8: present your reasoning for the local insolation/organic proxy age model tuning. It seems reasonable, but there should be more justification than just "other studies do it".

*I changed the order of the paragraph to lead with prior work/interpretation on this site, and the new dataset, in order to emphasize these and elaborate a little more. Examples of other studies then follow.*

141: was not were

142 replace "-" with "to"

146: Line beginning with "We hypothesize" belongs with next paragraph.

150-1 explain why this correlation suggests it.

155: alge are the source of organics? Provide some context. Also, insolation does not equal "available light", which can be influenced by other parameters like water clarity and ice cover. Do you mean potential light intensity? I think it might be better to rephrase this as "Because we expect light intensity reaching Baldwin Lake to be a primary control on algal organic matter production, we use local (30°N) summer insolation as a proxy for light intensity to establish age estimates for organic matter peaks and troughs".

158 "...possible other influences on organic matter production..." (again, be clear what you are referring to so the reader doesn't have to try to guess.)

*This section ("Chronologic Control") has been substantially rewritten to clarify the approach, and be clear about underlying assumptions made for the age model. I also addressed the concern from line 208 here about the immediate response to insolation we assume, vs. the ~3 kyr lag established for the Great Basin (about More detail below under that comment.)*

159 where not were.

*edited*

167: what are "default priors" and how are they relevant? This may be clear to a BACON user, but not to all readers.

*Thanks for this suggestion. This level of detail did not seem the norm in other literature using Bacon modeling, but since this is an unusually long core (and unusual use of Bacon), these details have now been included. I've also cited the paper that originally set the default priors for accumulation rates. Bacon suggested some alternatives for core section and memory, so I was clear in the text that we used these.*

170-1: rewrite "We interpreted the presence of a hiatus at 2596 cm because of a sharp break..."

*Rewritten, though with a different syntax (I noted a few other words/phrases that didn't make sense)*

173: "modern" means the age is certain, so as-written this is a non-sequiter. What you are probably referring to is "the uppermost sediments have an uncertain age" because of the lack of information on when the lake dessicated.

*Sentence has been rewritten with suggestions (and elimination of word "modern")*

183 how much longer? Provide numbers.

*A sentence was added to note the uppermost-dated horizon from the prior study (~20.3 ka at ~114 cm, compared to new results of ~11.9 ka at 152 cm)*

200: add period

*done*

208: Paleotemperature lagged insolation in the southwest by a few thousand years, but you are assuming without presenting any evidence that they do not. Why?

*There is not yet enough evidence that the drivers (e.g. boreal insolation with a millennial-scale lag) and processes that produce this in the Great Basin and Southwest are appropriate for California sites. In recent literature, local or subtropical insolation is*

*typically invoked for comparison with California paleorecords. The assumption in these studies is that there is an immediate response, or it is noted that age uncertainties are too large at present to detect a lag.*

*This description/argument has been added to the text, with supporting citations. I acknowledged that nearby physiographic regions (i.e. Great Basin) demonstrated a ~3 kyr lag with insolation earlier, in the "Methods: Chronologic Control" as part of the rationale for the age model, and why we used tie-points with no lag. I have added language (again, in this earlier section) that this is a set of assumptions supporting a first-pass interpretation of climate drivers and an age model (open to revision with future work on California paleorecords that can produce better-resolved chronologies prior to the LGM).*

211: coincided with not corroborated. Also "low dry density"? It isn't clear.

*Suggested word change made, and dry density (which has low values here) clarified.*

216-8: provide evidence supporting this interpretation.

*No concrete sedimentary evidence for this interpretation, so language has been tempered to indicate this is our hypothesis for a process that could produce low values (despite initial expectations for higher values).*

221: change to "We interpret relatively higher values of Ti, and in part, Fe, to phases of increased detrital, non-biogenic sediment deposition".

*Edited to reflect changes*

222-5 I don't understand how Ca and Mg/Ti are linked, or should this sentence be split in two?

*Ca and Mg/Ti are generally phased in this system and co-occur, but this comment is correct to point out that their interaction with each other is unknown. I have split this into separate sentences.*

229: re-write: "Taken together, we interpret the increased .... to reflect a warmer and ventilated lake. This warming may have also resulted from shallowing."

*Suggestions have been incorporated*

231: what evidence is there for anoxia?

*Good pollen preservation (and the smell!). However, these are lines of evidence that have continually been problematic to mention in this ms (see comments re. line 276). Sentence has been changed to suggest that anoxia is possible when the trace elements*

*mentioned in prior sentence are all low, yet organic matter values indicate productivity (phytoplankton deposition -> bacterial decay which depletes oxygen).*

235: rewrite "A luminescence age of xxx yr BP from a depth of yyy cm shows that sediment deposition at the base of the core began in MIS 5e..."

*Rewritten, though suggested syntax had to be adjusted to note there are two possible age ranges, depending on at which temperature the signal was measured.*

245: provide evidence to support this statement.

*Most supporting evidence for this statement in prior sentence – I have added additional evidence, and made the transition between sentences more clear.*

254: "indicate" not "indicates"

*edited*

273: change "suppressed" to "show low concentrations"

*edited*

276: provide citation for pollen preservation observation.

*I eliminated mention of the fossil pollen. Manuscript about it is not yet submitted to provide a citation, and Reviewer #2 had also noted this would need elaboration in this work.*

279: should read "organic matter concentrations"

*Edited*

288: should read "One possible interpretation for this high MS excursion is an increase (decrease?) in reducing conditions..."

*Edited to include this language (and clarified that reducing conditions decrease as a possible explanation for a high magnetic signal.*

290-1 should read "Shallow-water indicators Ca, CaCO<sub>3</sub>, and Mn:Ti increased suddenly around 12 ka, after which time Baldwin Lake likely transitioned to an intermittent, playa surface as summer insolation rose from 23 to 11 ka".

*Text edited to combine sentences and reflect the suggested syntax.*

301-2: does Owens lake have the chronology to make this statement? Or is it assumed based on visual curve matching?

*Sentence removed; likely a carry-over from prior draft where these data re. Owens Lake were shown (and subsequently removed, due to age model concerns expressed by both reviewers).*

305-8: what evidence? This seems to be circular, as there is not an independent chronology for the core to detect a difference between local insolation and paleotemperature (which lags insolation).

*Language here has been simplified, though I did not substantially change content. The statement (from earlier in the manuscript) that organic matter is a relative indicator of paleotemperature throughout the basin's history was eliminated in these revisions.*

320-4: these sentences need to be re-written clearly.

*These have been rephrased, along with a few of the subsequent sentences, for clarity. Basically we want to make a comparison between two periods of high summer insolation (over 510 W/m<sup>2</sup>) and explain why the site desiccated in the Early Holocene (but not before), with basin infilling likely playing a role.*

354: "... in Baldwin Lake's proxies for paleoproductivity (BSi and organic content) and temperature (what proxy?..."

*rephrased, and "temperature" eliminated based on rationale described above.*

400 "close to"? and 401 "at sites 1014..."

*both fixed*

438 "The Great Basin...."

*fixed*

498: "High-temperature low SST" doesn't make any sense.

*This has been rephrased*

---

Reviewer #2: This paper has been improved in many ways over the original submittal.

**SuppData\_SedDescription**

[Click here to download Supplementary Data: SuppInfo\\_SedDescription.docx](#)

**SuppData**

[Click here to download Supplementary Data: BDL12\\_DataForQSR\\_Mar2017.xls](#)